



TIDAL POWER GENERATION USING DFIG

By

Daniel Oluwatimilehin Obaleye

Supervisor: Asst. Prof. Dr. Hacer Şekerci

Submitted in fulfillment of requirements for the degree of Master's of Science (MSc.)

ELECTRICAL AND ELECTRONICS ENGINEERING DEPARTMENT,

FACULTY OF ENGINEERING,

GRADUATE SCHOOL OF NATURAL AND APPLIED SCIENCES,


YASAR UNIVERSITY, IZMIR, TURKEY.

NOVEMBER 2015


I certify that I have read this thesis and that in my opinion it is fully adequate, in scope and in quality, as a thesis for the degree of Master of Science.

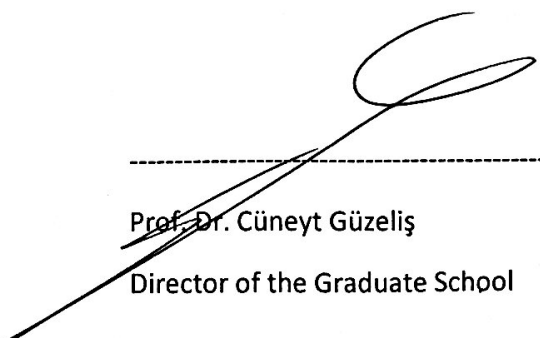

Asst. Prof. Dr. Hacer ŞEKERCİ (Supervisor)

I certify that I have read this thesis and that in my opinion it is fully adequate, in scope and in quality, as a thesis for the degree of Master of Science.


Asst. Prof. Dr. Emrah BIYIK

I certify that I have read this thesis and that in my opinion it is fully adequate, in scope and in quality, as a thesis for the degree of Master of Science.


Asst. Prof. Dr. Nalan ÖZKURT



Prof. Dr. Cüneyt Güzeliş
Director of the Graduate School

TABLE OF CONTENT

Cover Page	i
Clarification and Certification	ii
Table of Contents	iii
Acknowledgement.....	v
Dedication	vi
Index Of Figures.....	vii
Index Of Tables	ix
Index Of SymbolsAnd Abbreviations	x
Abstract.....	xii
Ozet	xiv
Chapter One	1
1.0 Historical Background Of Tidal Power	1
1.1 Thesis Summary.....	2
Chapter Two.....	3
2.0 Literature Review.....	3
2.1 Fundamental Conception Of Tides.....	4
2.2 The Concept Behind Two High Tides And Two Low Tides.....	5
2.3 Theory Behind Tidal Force And Differential Tidal Force	6
2.4 Reason For High Tide	10
2.5 Tidal Power Generating Methods And Types Of Tidal Turbines	11
2.6 Advantages And Disadvantages Of Ocean Tidal Power	21
2.7 Tidal Power Locations	22
2.8 Environmental Effect Of Tidal Power Generation	25
2.9 The Economics Of Tidal Power.....	27
Chapter Three	30
3.0 Modeling and Simulation Of 6 MW DFIG Tidal Turbine System For Different Fault Conditions	30
3.1.1 Description Of The Tidal Generation System	30
3.1.2 Tidal Turbine Modeling.....	44
3.1.3 Modeling Of DFIG.....	46
3.1.4 Back To Back AC/DC/AC Converter Modeling.....	50
3.1.5 Rotor Side Converter Control System	51
3.1.6 Grid Side Converter Control System	52
3.1.7 Tidal Turbine Protection Block	53
3.1.8 Tidal Turbine Data Acquisition System	53
3.1.9 Grid Data Acquisition.....	54
3.2.0 Simulation Results.....	55
3.2.1 Summary Of Analysis.....	75

Chapter Four	78
4.0 Conclusion	76
References	79

ACKNOWLEDGEMENT

Foremost, I would like to express my sincere gratitude to God the greatest for creating, upholding and strengthen me always. All thanks goes to my advisor Asst. Prof. Dr. Hacer Şekerci for the continuous support of my MSc. study and research, for her patience, motivation, enthusiasm, and immense knowledge. Her guidance helped me in all the time of research and writing of this thesis. I could not have imagined having a better advisor and mentor for my MSc. study. Besides my advisor, I would like to thank the rest of my lectures: Asst. Prof. Dr. Nalan Ozkurt, Assoc. Prof. Dr .Mustafa Seçmen and Prof. Dr. Mustafa Gündüzalp, for their encouragement, insightful comments, and hard questions.

I must acknowledge the beauty that makes me happy- my best friend, Arewa Eso Olabisi Rosemary, without whose love and encouragement. I would not have finished this thesis.

Last but not the least, I would like to thank my family: my parents Prof. and Mrs Obaleye, for giving birth to me at the first place and supporting me spiritually, morally, and financially throughout my life. My special appreciation goes to my wonderful siblings and my two nieces; Dr. (Mrs) Oluwaseyi Mercy Obaleye-Bamigboye, Dr. James Obaleye, Miracle Obaleye, Peter Obaleye, Inioluwa Bamigboye and Toluwani Bamigboye.

DEDICATION

I dedicate my MSc. degree to God almighty, my parents, siblings, and the Eso family.

Most importantly to my beloved late grandmother “Iyaonisu” who died year 2014. May her soul rest in perfect peace.

INDEX OF FIGURES

Figure 2.1 Person at point A experiences a tidal bulge due to the gravitational attraction of moon	17
Figure. 2.2. Spring tide	17
Figure 2.3. Neap tide.....	18
Figure 2.4 Newtonian conception of tidal force.....	18
Figure 2.5. Gravitational attraction of earth due to the attraction of moon	20
Figure 2.6. Reason responsible for high tide	22
Figure 2.7 Tidal Stream Generator	23
Figure 2.8 Tidal Stream Generation.....	26
Figure 2.9 The normal tidal curve and the modified tidal curve in the head pond above a tidal barrage in an estuary for (a) dual cycle generating and (b) ebb only generation.....	29
Figure 2.9.1 (a) the right angle to oceans tides.....	30
Figure 2.9.1 (a) the right angle to oceans tides.....	30
Figure 2.9.2 Ocean tides.....	33
Figure 2.9.2 Locations with the most potential for tidal energy	36
Figure 3.1.0 Mechanical Characteristics of Turbine	42
Figure 3.1.1 SIMULINK Model of 6 MW Tidal Power System	43
Figure 3.1.2 Power Coefficient vs. λ Characteristics	44
Figure 3.1.3 SIMULINK Model of Tidal Turbine.....	45
Figure 3.1.4 d q Axis Equivalent Circuit of DFIG	46
Figure 3.1.5 Back to Back AC/ DC/ AC Converter.....	50
Figure 3.1.6 Rotor Side Converter Control System.....	51
Figure 3.1.7 Grid Side Converter Control System.....	52
Figure 3.1.8 Tidal Turbine Protection Block.....	52
Figure 3.1.9 Tidal Turbine Data Acquisition System.....	53
Figure 3.2.0 Grid Data Acquisition System.....	54
Figure 3.2.1(a) Grid Voltage-Normal.....	55
Figure 3.2.1(b) The tidal site output voltage and the voltage in 25 kV line.....	55
Figure 3.2.1 (c) Voltage in 25kV Line-Normal.....	56
Figure 3.2.1 (d) Vdc-Normal	56
Figure 3.2.1 (e) Generated Real Power-Normal	57
Figure 3.2.1 (f)Generated Reactive Power-Normal.....	57
Figure 3.2.1 (g). Real Power In 25 kV Line-Normal	58
Figure 3.2.1 (h) Reactive Power in 25 kV Line-Normal.....	58
Figure 3.2.2 (a) Grid Voltage-Phase A to Ground Fault.....	59
Figure 3.2.2 (b) Phase A Voltage drop fault.....	59
Figure 3.2.2 (c) Voltage in 25kV Line-Phase A to Ground Fault.....	60
Figure 3.2.2 (d) Vdc-Phase A To Ground Fault.....	60
Figure 3.2.2 (e) Generated Real Power-Phase A to Ground Fault.....	61

Figure 3.2.2 (f) Generated Reactive Power-Phase a to Ground Fault	61
Figure 3.2.2 (g)Real Power in 25kV Line Phase A to Ground Fault	61
Figure 3.2.2 (h) Reactive Power in 25kV line-phase a to ground fault.....	62
Figure 3.2.3 (a)Grid voltage-phase A B fault	62
Figure 3.2.3 (b)Phase A Voltage fault during drops.....	63
Figure 3.2.3 (c)Voltage in 25kV line-phase A B fault	63
Figure 3.2.3 (d) Vdc Phase A B fault	64
Figure 3.2.3 (e)Generated real power phase A B fault.....	64
Figure 3.2.3 (f) Generated reactive power phase A B fault.....	65
Figure 3.2.3 (g) Real power in 25kV line phase A B fault.....	65
Figure 3.2.3 (h) Reactive power in 25kV line phase A B fault.....	66
Figure 3.2.3 (i) Tidal Speed	66
Figure 3.2.4 (a) Grid Voltage Phase A B to ground fault	67
Figure 3.2.4 (b) Phase B voltage of the tidal site drops under fault	67
Figure 3.2.4 (c) Voltage in 25kV line phase A B to ground fault.....	68
Figure 3.2.4 (d) Vdc Phase A B to ground fault	68
Figure 3.2.4 (e) Generated real power phase A B to ground fault.....	69
Figure 3.2.4 (f) Generated reactive power phase A B to ground fault.....	69
Figure 3.2.4 (g) Real power in 25kV line phase A B to ground fault	70
Figure 3.2.4 (h) Reactive power in 25kV line phase A B to ground fault	70
Figure 3.2.5 (a) Grid voltage-symmetric fault.....	71
Figure 3.2.5 (b) Phase A, B and C voltages of the tidal site drops	71
Figure 3.2.5 (c) Voltage in 25 kV line-symmetric fault.....	72
Figure 3.2.5 (d) Vdc-Symmetric fault	72
Figure 3.2.5 (e) Generated real power-symmetric fault.....	73
Figure 3.2.5 (f) Generated reactive power-symmetric fault	73
Figure 3.2.5 (g) Real power in 25kV line-symmetric symmetric fault	74
Figure 3.2.5 (h) reactive power in 25kV line-symmetric fault.....	74

INDEX OF TABLES

Table 3.1 Definition of subscripts.....	46
Table 3.2 Definition of parameters in model.....	47

INDEX OF SYMBOLS AND ABBREVIATIONS

S/N	Unit name	UnitSymbol
1.	US	United States
2.	kV	kilo volt
3.	MW	Megawatt
4.	PV	Photovoltaic
5.	DFIG	Doubly-Fed Induction Generator
6.	V	Volt
7.	MVA	Megavolt-amps
8.	PF	Powerfactor
9.	Pu	Per unit
10.	Ms	Mass of Sun
11.	Mm	Mass of Moon
12.	Ds	Distancefromearthto sun
13.	Dm	Distance from earth to moon
14.	W	Watt
15.	Kg/cm ³	Density of medium
16.	(m/s) ³	Cubic metre per second
17.	A	Cross-sectionalarea
18.	ρ	Density of water
19.	Km ²	Kilometer square
20.	DTP	DynamicTidalPower
21.	GW	Gigawatt
22.	MWh	Mega watthour
23.	Emfs	Electromagnetic
24.	£	Pounds
25.	IGBT	Insulatedgatebipolar transistor
26.	AC	Alternatingcurrent
27.	DC	Direct current
28.	m/s	Metre persecond
29.	Hz	Frequency
30.	β	Pitch angle
31.	Cp	Powercoefficient
32.	Tm	Electromagnetictorque
33.	Cr	Rotor converter
34.	Cgrid	Gridsideconverter
35.	Idgc	Currentreference
36.	Vgc	Voltagephase
37.	Vdc	Voltage of directcurrent
38.	MVAR	Mega volt-ampere reactive
39.	G	Gravitationalattraction of earth
40.	F _A	Rotationalforce
41.	Me	Mass of earth
42.	F _m	Force duetomoon
43.	F _s	Force dueto sun
44.	T _s	Tide duetotheeffect of sun

45.	T_{μ}	Tidal due to the effect of moon
46.	ebb	The movement of tide out to sea
47.	pf	Power factor
48.	€	Euro
49.	mph	Mile per hour

ABSTRACT

Concern over global climate change has led policy makers to accept the importance of reducing greenhouse gas emissions. This in turn has led to a large growth in clean renewable generation for electricity production. Much emphasis has been on wind generation as it is among the most advanced forms of renewable generation, however, its variable and relatively unpredictable nature result in increased challenges for electricity system operators. Tidal generation on the other hand is almost perfectly forecastable and as such may be a viable alternative to wind generation. This thesis paper shows the important of Tidal power over other sources and it's generation using DFIG.

This thesis is analyzed based on the following configuration;

A 6 MW tidal power site having four, 1.5 MW tidal turbines connected to a 25 kV distribution system which ensures power to a 120 kV grid through a 30 km, 25 kV feeder line. A 2300V, 2 MVA plant with a motor load (1.68 MW induction motor at 0.93 pf) and of a 200 kW resistive load which is also linked into the same feeder. Both tidal turbine and motor is attached to a protection system which was used to monitor voltage, current and machine speed. DFIG DC link voltage is also monitored. Tidal turbines used an induction generator having a wound rotor and an AC/DC/AC IGBT based PWM converter. The stator winding is also linked directly to the 50 Hz grid and the rotor is fed at variable frequency through the AC/DC/AC converter. DFIG technology was also used for extraction of maximum energy from the tides for low tidal speeds through optimization of turbine speed, while lowering turbine mechanical stresses during heavy tides. The turbine's optimum speed used to produce maximum mechanical energy for a given tidal speed which is directly proportional to tidal speed. The rotor runs at sub synchronous speed for tidal speeds will also be lowered at 10 m/s and at super synchronous speeds for higher tidal speeds.

The simulation of 6MW tidal site was carried out for normal condition and at different types of faults introduced on the 25kV line. They are carried out as follows;

- a) For normal conditions, at a tidal speed of 13m/s.
- b) For a phase A to ground fault in the 25 kV line for $t=5$ to 5.1 seconds.
- c) For a phase A and B fault in the 25 kV line $t=5$ to 5.1 seconds.

- d) For a phase A and B to ground fault in the 25 kV line $t=5$ to 5.1 seconds.
- e) For a symmetric fault in the 25kV line for $t=5$ to 5.1 seconds

ÖZET

Küresel iklim değişikliği konusundaki endişe politikacıların sera gazı emisyonlarının azaltılmasının önemini kabul etmelerini sağlamıştır. Bu da elektrik üretimi için temiz ve yenilenebilir bir çağ başlatmıştır. Bu vurgu şimdiye kadar rüzgar üretimindeydi ki bu yenilenebilir üretimin en gelişmiş biçimlerinden biridir. Buna rağmen elektrik sistem operatörleri için bağımsız değişkenlerin öngörülemez doğası sonucu artan zorluklar bulunmaktadır.

Bir diğer taraftan dalga enerjisi mükemmel bir şekilde öngörülebilir ve rüzgar enerjisine alternatif olabilmektedir. Bu tez diğer enerji kaynaklarına kıyasla dalga enerjisinin gücünün önemini göstermektedir ve bu enerji için DFIG kullanılır.

Bu tez, aşağıdaki şekilde analiz edilmiştir:

A 6 MW dalga enerjisi dört adet 1,5 MW dalga türbinine sahiptir ve bunlar 25 KVlık dağıtım sistemine bağlıdır. Bu 25 KVlık besleme hattı üzerinden 120 KV şebekeye 30 km yol olarak güç sağlar. A 2300 V, 2MVA tesisi motor ağırlığı ile (1,69 MW endüksiyon motoru 0,93 PF) ve 200 KW lık direnç gücü ki bu ayrıca aynı besleyiciye bağlıdır.

Dalga türbini ve motor voltaj, akım ve makine hızını izlemek için kullanılan bir koruma sistemine takılır. FFIG DC bağlantı voltajı da ayrıca izlenir. Dalga türbinleri PWM dönüştürücüsüne dayanan AC/D/AC/İGBM ve yaralı pervaneye sahip endüksiyon jeneratörü olarak kullanılır. Stator (gövde) sargısı ayrıca 50 Hzlık şebekeye bağlıdır ve pervane AC/DC/AC dönüştürücü sayesinde değişken frekansla beslenir.

FIG teknolojisi güçlü dalgalar sırasında türbin mekanik zorlamalar yaşarken ve aynı zamanda da türbin hızının maksimum enerjisi ortaya çıkarmak için düşük dalga hızının optimizasyonunu sağlamak amacıyla kullanılmıştır.

Türbinin optimum hızı dalga hızı ile doğrudan orantılı olan belirli bir dalga hızı için maksimum mekanik enerjisi üretmek için kullanılır. Pervane hızı dalga hızı için süper alt senkron hızı ile çalışır. Bu hız ayrıca 10 m/s yüksek süper senkron hızlarında en yüksek dalga hızı olacaktır.

Normal şartlarda uygulanan 6 MW simülasyonu ve 25 KVlık hattaki farklı tip hatalar tanıtıldı. Bunlar aşağıdaki gibi uygulamalardır;

- a) Normal şartlarda, bir dalga hızı 13 m/s'dir.
- b) Bir faz için A zemin hatasında 25 kv hat için $t = 5, 5.1$ saniye
- c) Bir faz için A ve B hatalarında 25 kv hat $t = 5, 5.1$ saniye

- d) Bir faz için A ve B zemin hatasında 25 kv hat için $t= 5, 5.1$ saniyede
- e) Bir simetrik hata için 25 kv hat için $t=5, 5.1$ saniyede

CHAPTER ONE

1.0 HISTORICAL BACKGROUND OF TIDAL POWER

Due to the quest to reduce the use of fossil fuel to generate electricity which causes green house effect. A lot of research has been done to find other means of power generation especially renewable energies [1]. One of the most effective and efficient renewable sources is tidal power. The use of tidal power originated in around 900 AD when early civilizations constructed tide mills. These mills used the force of the tide to turn a waterwheel, which in turn was used to grind grain into flour [2]. Britain and France are using the tidal power concept since 11th century for milling grains [3]. The first study of large scale tidal power plants was initiated by the US Federal Power Commission in 1924 which would have been located if built in the northern border area of the US state of Maine and the south eastern border area of the Canadian province of New Brunswick, with various dams, powerhouses and ship locks enclosing the Bay of Fundy and Passamaquoddy Bay. Nothing came of the study and it is unknown whether Canada had been approached about the study by the US Federal Power Commission [4]. The world's first large-scale tidal power plant (the Rance Tidal Power Station) became operational in 1966 [5]. The facility is located on the estuary of the Rance River, in Brittany [6]. With a peak rating of 240 Megawatts, generated by its 24 turbines, it supplies 0.012% of the power demand of France [7]. The second tidal barrage was put in service at Annapolis Royale Nova Scotia, Canada in 1982 in order to demonstrate the functioning STRAFLO turbine, invented by Escher-Wyss of Switzerland and manufactured by GE in Canada. This 16 MW turbine has some difficulties with clogging seals necessitating two forced outages, but has been functioning without interruption since its early days. There are approximately 10 small barrages scattered throughout the world, but they are not intended for commercial power generation. For example there is a 200kW tidal barrage on the river Tawe in Swansea Bay. China has several tidal barrages of 400kW and less in size [8].

The past decade has seen a major growth in renewable energy, driven by policies addressing climate change and efforts to sustainably diversify electricity supplies. As one of the most advanced forms of renewable generation, much emphasis has been on wind, which has grown from 9,660MW installed worldwide in 1998 to over 120,800 MW in 2008 [9]. However, wind output is variable and relatively unpredictable resulting in increased challenges for power system

operators in balancing electricity supply and demand at all times. Tidal generation has a significant advantage over many other renewable as it can be almost perfectly forecasted over long time horizons. Thus, incorporating tidal generation into an electricity system should be less challenging than for other forms of renewable generation [10].

1.1 THESIS SUMMARY

This thesis gives an insight to different methods of tidal generation. It also presents the complete modeling and real-time simulation of tidal turbine driven DFIG which feeds ac power to the utility grid. I will also envisage the use of driven DFIG to extract maximum energy from ocean tides at low tidal speed by optimizing the turbine speed, while minimizing mechanical stresses on the turbine during gusts of different levels of tides.

The first chapter focuses on the historical background of tidal power. While the second chapter emphasizes on the fundamental conception of tides, the concept behind the two high tides and two low tides, the theory behind tidal force, differential tidal force, reason for high tides, the advantages and disadvantages of ocean tidal power generation. Furthermore, chapter three concentrates on the modeling and simulation of tidal power site at different fault conditions. While the rest of the thesis anchors on the conclusion and future research work.

Past research focuses on the use of permanent brushless DC motor. The magnetic fields produced as a result of the spiral movement of the magnet within the component is that which produces electricity. Brushed DC motors can be varied in speed by changing the operating voltage or the strength of the magnetic field. Depending on the connections of the field to the power supply, the speed and torque characteristics of a brushed motor can be altered to provide steady speed or speed inversely proportional to the mechanical load.

CHAPTER TWO

2.0 LITERATURE REVIEW

Tidal power, also called tidal energy, is a form of hydropower that converts the energy of tides into useful forms of power, mainly electricity. Although not yet widely used, tidal power has potential for future electricity generation. Tides are more predictable than wind energy and solar power. Among sources of renewable energy, tidal power has traditionally suffered from relatively high cost and limited availability of sites with sufficiently high tidal ranges or flow velocities, thus constricting its total availability. However, many recent technological developments and improvements, both in design (e.g. dynamic tidal power, tidal lagoons) and turbine technology (e.g. new axial turbines, cross flow turbines), indicate that the total availability of tidal power may be much higher than previously assumed, and that economic and environmental costs may be brought down to competitive levels [11].

The electrical layout and modeling approaches used in tidal in-stream systems are similar to those used for wind and offshore-wind systems. The speed of water currents is less than wind speed, while water density is higher than air density and as a result wind turbines operate at higher rotational speed and lower torque than tidal in-stream turbines which operate at lower rotational speed and high torque. Therefore in some tidal instream system designs the mechanical coupling between the turbine and generator is done through a gearbox. Also the system collecting electricity may be different and this will influence the choice of methods used in stability studies and the connection of the overall system, but tidal currents are easier to predict than wind speed.

A detailed FSWT model for stability studies with stator transient included has been addressed in the PhD thesis by Akhmatov [12]. The inclusion of the stator current transient allows an accurate speed deviation prediction. A DFIG wind turbine model for power system stability studies was also proposed in the same thesis with the stator flux transient included. By doing so, the FRT scheme can be modeled in detail. However, this representation poses difficulties in the model implementation into positive sequence fundamental frequency simulation tools due to a very

small time step requirement and incompatibility with standardized power system components. A reduced order model of a DFIG wind turbine model has been introduced in [13] where the stator transient is neglected during a normal operation. However, the involvement of current a controller still requires high simulation resolution. A simplified model of a DFIG wind turbine that is compatible with the fundamental frequency representation was proposed in [14]. The DFIG was modeled by neglecting both stator and rotor flux dynamics. This model is equivalent to a steady state representation, while the rotor current controller is assumed to be instantaneous. Consequently, iteration procedure - which is not preferable in the model implementation - is needed to solve algebraic loops between the generator model and the grid model. By introducing time lags, which represent delays in the current control, the algebraic loops are avoided [15]. However, the maximum power tracking (MPT) in this model is assumed to be a direct function of incoming wind speed, whereas in common practice, the MPT is either driven by the generator speed or the generator power output. Another simplified DFIG model was presented in [16]. According to this model, the generator is simply modeled as a controlled current source, thus the rotor quantities are omitted. The things that are missing from the proposed simplified models mentioned earlier are that the rotor current limiters are excluded and the FRT schemes are not clearly modeled. Representations of detailed FCWT models for power system studies are presented in [12]. In these papers the generators are modeled in detail. Consequently, these models require very small time step and thereby complicate the implementation in a standardized fundamental frequency simulation tool. A simplified of an FCWT model was proposed in [16].

Several remarks can be drawn from the review of previous works:

- Each model presented in the papers is associated with a particular type of controller and uses a particular FRT scheme if it exists. The sensitivity and influences of different control and FRT schemes on wind turbine responses have not been treated in the papers.
- The FRT schemes are often excluded from the simplified models, whereas the FRT schemes substantially characterize the response of wind turbines during grid faults.
- Most of the simplified models are not validated against more detailed models or measurement data. This leads to uncertainty in the accuracy of the model responses.

2.1 FUNDAMENTAL CONCEPTION OF TIDES

From the fundamental conception of tide it is known that tide occurs due to the gravitational attraction of moon. From figure 2.1 it is seen that anybody in Earth at point A will experience a tide due the gravitational attraction of moon. So any body at point A will experience only one tide, because earth rotates around its own axis one time per day [17]. But this theory is completely wrong. Because earth is rotating around its own axis, there will be one high tide and one low tide per day. But again the theory is wrong. Correct theory is, there are two tides per day which are two high tides and two low tides.

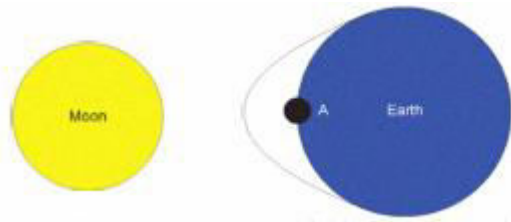


Figure 2.1 Person at point A experiences a tidal bulge due to the gravitational attraction of moon

2.2 THE CONCEPT BEHIND TWO HIGH TIDES AND TWO LOW TIDES

It is seen that tide occurs due to the gravitational attraction of moon. But moon is not the only element that causes tide. The effect of sun also causes tide. When sun and moon lines up with earth than it is called new or full moon phase. The gravitational forces of the Moon and the Sun both contribute to the tides. At this time the gravitational pool of moon and sun are combined and high tides become very high and low tides become very low. This phenomenon is known as Spring tide. Spring tides are very strong tide [18].

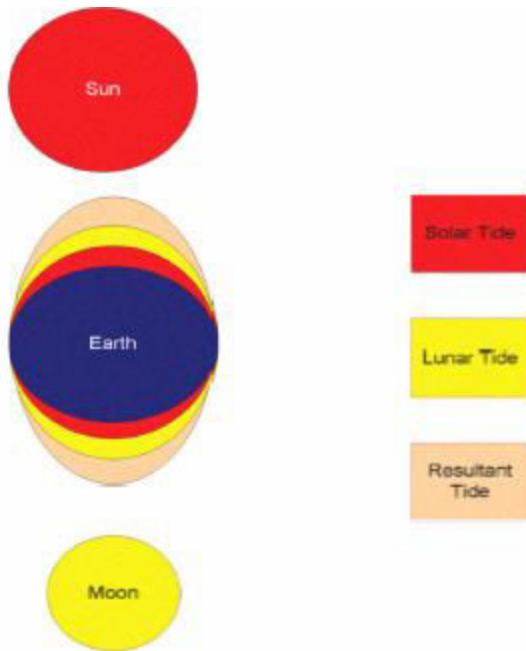


Figure 2.2. Spring tide

When sun and moon lines up with earth in opposite side than it is called quarter moon phase. During the moon's quarter phases the sun and the moon work at right angles, causing the bulges to cancel each other. The result is a smaller difference between high and low tides. This phenomenon is called neap tide [19]. They occur when the gravitational forces of Moon and the Sun are perpendicular to one another. Neap tides are generally weak tides.

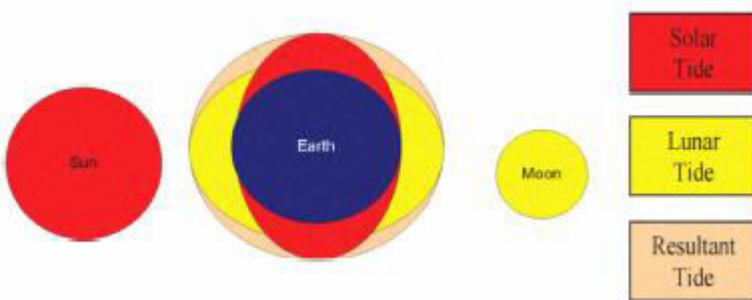


Figure 2.3. Neap tide

2.3 THEORY BEHIND TIDAL FORCE AND DIFFERENTIAL TIDAL FORCE

Different scientist in different time gave the conception of tidal force. But the conception of tidal force was correctly given by Newton. To get the correct conception one illustrated object is

considered at the top of the earth surface which is falling but not actually falling towards the earth surface and at the same time two points X and Y is considered as shown in Fig. 2.4. Force experienced at point X will have a natural tendency to fall and the force will be smaller due to smaller acceleration. But force experienced at point Y will be larger because of the greater acceleration. As a result there will be an elongation in both direction and the force which will be occurred, is tidal force. Now if the round objects as in Fig. 2.4 is considered as earth and because the earth is solid and the ocean part is liquid the ocean water will be bulged in two directions due to the attraction of tidal force [20].

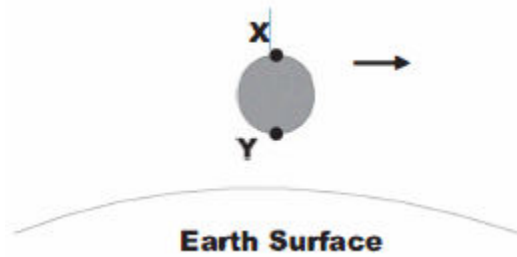


Figure 2.4. Newtonian conception of tidal force[16]

From the common point of view it is understood that tidal effect due to the moon is stronger than tidal effect due to the sun [21]. Because sun is far away from earth and because the moon is nearer to the earth, its gravitational pull is larger. But the conception is not at all correct. Let us consider,

Force due to sun,

$$F_s = \frac{GMeMs}{D_s^2} \quad (1)$$

Force due to moon,

$$F_m = \frac{GMeMm}{D_m^2} \quad (2)$$

$$\frac{M_s}{M_m} = 26800000 \quad (3)$$

$$\frac{D_s}{D_m} = 390 \quad (4)$$

$$\frac{F_s}{F_m} = \frac{M_s}{M_m} \times \frac{D_m^2}{D_s^2} \quad (5)$$

$$\frac{F_s}{F_m} = \frac{26800000}{390^2} \quad (6)$$

$$\frac{F_s}{F_m} = 176.19$$

$$\frac{F_s}{F_m} \cong 176$$

$$F_s = 176 \times F_m \quad (7)$$

Attraction due to the sun is 176 times stronger than attraction due to the moon. It is seen from the equation (1) that attraction due to the sun is 176 times larger due to the moon. So tidal effect due to the moon is stronger than tidal effect due to the sun is wrong. But the thing is to consider that tidal force is not the reason for tides. The reason is differential force between the two points X and Y (Fig. 2.4) along the diameter of the earth [22].

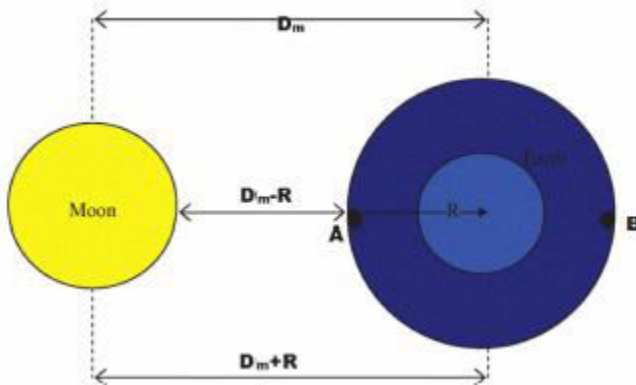


Figure 2.5. Gravitational attraction of earth due to the attraction of moon

Let us consider, Attraction due to the moon at Point A,

$$F_A = G \frac{M_m \mu}{(D_m - R)^2} \quad (8)$$

Attraction due to the moon at Point B,

$$F_B = G \frac{M_m \mu}{(D_m + R)^2} \quad (9)$$

$$F_A - F_B = GM_m \mu \frac{(D_m + R)^2 - (D_m - R)^2}{(D_m - R)^2 - (D_m + R)^2} \quad (10)$$

$$= GM_m \mu \frac{D_m^2 + 2D_m R + R^2 - D_m^2 - 2D_m R - R^2}{(D_m^2 - R)^2}$$

$$= GM_m \mu \frac{4D_m R}{(D_m^2 - R)^2} \quad (11)$$

$$= GM_m \mu \frac{4R}{D_m^3 \left(1 - \frac{R^2}{D_m^2}\right)^2} \quad (12)$$

$$= F_A - F_B$$

$$= GM_m \mu \frac{4R}{D_m^3} \left[\text{The term } \frac{R^2}{D_m^2} \text{ can be ignored because it is much smaller than 1} \right] \quad (13)$$

$$\frac{R^2}{D_m^2} = \frac{1}{60} \quad (14)$$

Force responsible for tide due to the effect of moon is,

$$T_m = GM_m \mu \frac{4R}{D_m^3} \quad (15)$$

Force responsible for tide due to the effect of sun is,

$$T_s = GM_s \mu \frac{4R}{D_s^3} \quad (16)$$

Now, (15) ÷ (16)

$$\begin{aligned} \frac{T_m}{T_s} &= \frac{GM_m \mu \frac{4R}{D_m^3}}{GM_s \mu \frac{4R}{D_s^3}} \\ \frac{T_m}{T_s} &= \frac{GM_m \mu 4R}{D_m^3} \times \frac{D_s^3}{GM_s \mu 4R} \\ \frac{T_m}{T_s} &= \frac{M_m}{M_s} \times \left(\frac{D_s}{D_m}\right)^3 \\ \frac{T_m}{T_s} &= \frac{1}{26800000} \times (390)^3 \\ \frac{T_m}{T_s} &\cong 2.2 \\ \therefore T_m &= 2.2 \times T_s \quad (17) \end{aligned}$$

From the equation it is seen that tidal force due to the moon is 2.2 times larger than tidal force due to the sun. From equation (15) it is seen that the actual attraction due to the moon is much smaller than sun but from equation (17) it is seen that the differential attraction due the moon is 2.2 times than attraction due to the sun. This differential force is responsible for tide. So it can be said that there are two tidal bulges at the two sides of earth due to the attraction of moon and two tidal bulges at the two sides of earth due to the attraction of sun.

2.4 REASON FOR HIGH TIDE

To generate tidal power high tide is essential. Normally for tidal power generation minimum 1.5 m (4.9 feet) tidal variation is needed. Tidal variation means variation of tide from lowest point of the ebb tide to highest point of high tide. So for high tide specific topography is needed. From Fig. 1.6 it is seen that small bulges is approaching towards the shore line. As it pushes up water goes in to the estuaries and when there is low tide water goes down. So water is going in and coming out. It has its own natural oscillation and the tidal variation has its own natural oscillation [23]. When these two frequency matches there is a resonance. This resultant resonance causes large tide, for example more than 10 feet.

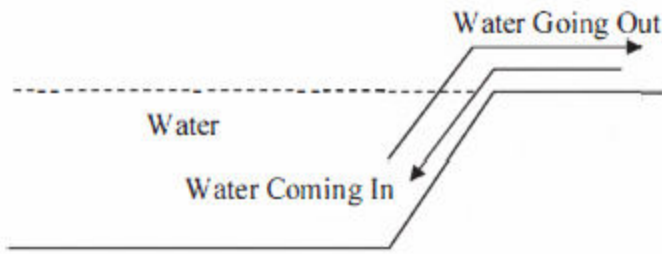


Fig. 1.6. Reason responsible for high tide.

2.5 TIDAL POWER GENERATING METHODS AND TYPES OF TIDAL TURBINES

Generating Methods: Tidal power can be classified into three generating methods: Tidal stream generator, Tidal barrage, Dynamic.

1. **A tidal stream generator** is a machine that extracts energy from moving masses of water, or tides. These machines function very much like underwater wind turbines, and are sometimes referred to as tidal turbines. Tidal stream generators are the cheapest and the least ecologically damaging among the three main forms of tidal power generation [23].



Fig. 2.7 Tidal Stream Generator

Tidal Stream is the name given to the horizontal flow of water through the oceans caused by the continuous ebb and flood of the tide, which as we know is the vertical up-down movement of the oceans water. Unlike water currents which are a continuous, unidirectional and form a steady horizontal movement of water flowing down a river or stream etc, a *tidal stream* or tidal current, changes its speed, direction and horizontal movement regularly according to the forces of the tide controlling it as shown in figure 2.7. Tidal stream generation is a non-barrage tidal scheme which extracts the kinetic energy (energy in motion) from moving water generated by the tides without altering the environment thereby making it a Hydrokinetic Energy system. At or near the coast, the ebb and flood of the tides causes the oceans waters to pile up resulting in a high tide along the beach, with some of this water being forced into tidal inlets, basins and estuaries while the majority is forced sideways along the shore. This movement of the tidal range amplified by geographical features along the coastline, focuses these tidal currents into a single predictable and concentrated form of renewable energy which we can exploit using a tidal stream generator. A tidal stream is usually stronger nearer to the coast where the sea water is naturally shallower causing the water to speed, than it is farther out in deeper depths [24].

Tidal Stream Generation is very similar in many ways to the principles of wind power generation. Horizontal turbine generators called “tidal turbines” or “marine current turbines” are placed on the ocean floor, the stream currents flow across the turbine blades powering a generator much like how wind turns the blades of wind power turbines. In fact, in some tidal stream generation areas the sea bed looks just like underwater wind farm with arrays of tidal stream generators covering large areas. The generated tidal electricity is then transmitted to the shore via long underwater electrical cables called *submarine cables*. These offshore tidal turbines can be either partially or fully submerged beneath the surface of the water, with partially submerged turbines being easier and less costly for maintenance. While tidal stream installations reduce some of the environmental effects of large man-made tidal barrages, major ocean currents like the Gulf Stream, travel at speeds significantly slower than the wind. However, as water is 800 times denser than air (which is why we can see water and not air), a single tidal generator sitting on the sea bed can provide a significant amount of ocean current energy at low tidal stream velocities which is far superior to wind, using similar or identical turbine technology. Since energy output varies with the density of the medium, (kg/cm^3) and the cube of the

velocity, (m³/s), we can see that a 10 mph (about 8.6 knots in nautical terms) ocean tidal current would have an energy output equal or greater than a 90 mph wind speed for the same size of turbine system. Therefore, even small increases in velocity can lead to substantial changes in the amount of available power and therefore, smaller faster rotating tidal turbine generators can be used in a ocean based tidal stream system.

As the kinetic energy content of a tidal stream flows per unit time, which is the same as the hydro power (P), the available energy can be calculated in terms of velocity (V), swept cross-sectional area (A) perpendicular to the stream flow direction, and the density of the water (ρ), which for sea water is approximately 1025 kg/m³. Providing the velocity is uniform across the cross-sectional area, at any instant in the tidal cycle the amount of energy available will be;

$$P = \frac{1}{2} \rho A.V^3 \quad (18)$$

This cubic relationship between velocity and power is the same as that for the power curves relating to wind turbines, but there are practical limits to the amount of power that can be extracted from tidal streams. Some of these limits relate to the design of the tidal stream turbines and the characteristics of the underwater resource.

Tidal Stream Generator Designs Unlike off-shore wind power which can suffer from storm or heavy sea damage, tidal or marine current turbines operate just below the sea surface or are permanently fixed to the sea bed. Most submerged tidal turbines essentially operate in the same way as a wind turbine and are fastened to the ocean floor, with water pushing the turbine instead of the wind. These turbines have an axis of rotation horizontal to the ground and operates like a traditional windmill consisting of a rotor, a gearbox, and an electrical generator. These three parts are mounted onto a steel support structure with the three main types of support being a gravity structure, a sunken piled structure or a tripod structure as shown [25].

Tidal Stream Generator Supports

For a sunken pile support, a single steel pile is driven deep into the sea bed with the tidal stream generator assembly attached to it. This tubular support is less stiff than other types and can flex under the downstream drag forces of the tidal waters when used in shallow waters. A gravity support generally uses a large heavy concrete block or blocks which sit on the sea bed as shown in figure 2.8. Due to the heavy weight of the concrete block, the structure is stiffer and therefore more resistant to flexing. A tripod or truss support uses a tubular frame with a much larger footprint positioned on the ocean floor to support the generator assembly. This type of system is used in oil and gas exploration so is a known technology [25].

Other tidal stream generator designs fixed to the ocean floor include: Reciprocating Tidal Stream Devices that uses a large hydrofoil similar to a whales flipper, which moves up and down parallel to the direction of the tidal stream instead of rotating blades, and Venturi Effect Tidal Stream Devices, where the tidal turbines are located inside a cylindrical duct, much like a fan housing. The tidal flow is funneled through this duct, which concentrates the flow producing a pressure difference causing a secondary water flow through the reaction turbine thereby improving efficiency [26].

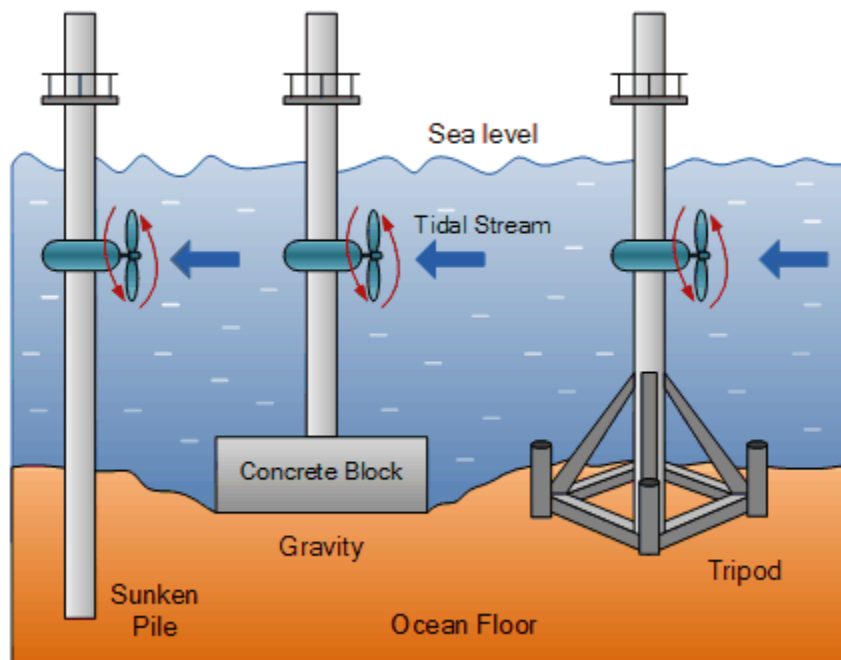


Fig. 2.8 Tidal Stream Generation

Also, there are several practical advantages in placing the tidal turbine inside a fan type duct, such as less dangers from the rotating blades to both aquatic marine life and divers as a safety grill or cover could be placed on the upstream opening which would also have the secondary advantage of preventing floating debris from being drawn or sucked into the turbine causing damage. The duct itself can provide shading and/or shelter for the reaction turbine from direct sunlight, preventing seaweed, algae growth or crustaceans forming on the blades and mechanism as they do on the underside of boats. Tidal streams are formed by the fast flowing horizontal currents of water caused by the ebb and flow of the tides with the profile of the sea bed causing the water currents to speed up, or slow down near the shoreline. Then tidal stream turbines can generate power on both the ebb and flow of the tide. One of the disadvantages of Tidal Stream Generation is that, as the turbines are submerged under the surface of the water they can create hazards to large sea mammals, navigation and shipping. Given the technical difficulties resulting from underwater corrosion, increased maintenance issues, weed growth on the blades, which could reduce their efficiency and stability concerns, other forms of alternative tidal stream generator designs are now being used. These include the tidal turbine being connected to a floating barge or ship on the water surface, essentially operating as an upside down horizontal turbine instead of fastening the turbines directly to the ocean floor [27].

There are numerous advantages to this type of tidal stream generator design, including easy maintenance and accessibility of the turbines, by simply removing or replacing them out of the water, and no costly steel supports or alterations to the ocean floor. Also, as the tidal turbines are located under a barge, pontoon or fixed directly to the hull of a ship, they can have their electrical connections and equipment mounted safely above and out of the water. Plus the supporting flotation device can be easily moved to stronger tidal stream areas if required, but they are limited by distance due to their umbilical electrical cable connected to the shoreline.

- 2. Tidal barrage** is a dam-like structure used to capture the energy from masses of water moving in and out of a bay or river due to tidal forces. Instead of damming water on one side like a conventional dam, a tidal barrage first allows water to flow into a bay or river during high tide, and releasing the water back during low tide. This is done by measuring

the tidal flow and controlling the sluice gates at key times of the tidal cycle [23]. Turbines are then placed at these sluices to capture the energy as the water flows in and out. Tidal barrages are among the oldest methods of tidal power generation, with projects being developed as early as the 1960s, such as the 1.7 megawatt KislayaGuba Tidal Power Station in KislayaGuba, Russia.

Tidal barrages work like hydroelectric dams except water needs to flow in both directions. The sluice gates are opened to allow the tide to flood into a basin (estuary, fjord or bay); at high tide the sluices in the barrage are closed and the tide outside falls. Once a sufficient height differential has occurred the turbines are opened and the contained water flows out through the turbines. This continues until the tide turns and the differential head is eroded. The sluices are then opened to allow the basin to refill. This operation method, known as ebb generation, generates the most power. It is also possible to generate power on the flood tide by refilling the basin through the turbines, while this generates power for more of the tidal cycle it generates less power in total as there is less of a differential head. Both tidal flows may be harnessed in dual mode devices [28]. Building a barrage across a bay/estuary will destroy the former benthic habitat in the construction footprint. Construction and decommissioning activities can result in impacts to adjacent intertidal areas if used for construction of caissons or as staging areas. The presence of a barrage also influences habitats upstream and downstream of the facility. Upstream under ebb only generation, the upper intertidal remains submerged for a longer period, there is then a steady fall in tide level until the tide starts rising again Fig 2.9. The former lower shore remains submerged. These changes will shift the balance between marine intertidal species, with upper shore specialists potentially being squeezed out. The retention of water also significantly alters the exposure of tidal flats to feeding birds although the resource in the tidal flats when they are exposed may increase in quantity and quality. The availability of alternative feeding/roosting sites is therefore often critical. Downstream of the barrage tidal range is often reduced close to the barrage but enhanced in other parts of the basin. The outflow will delay the falling tide from around mid-tide downward, such that the tide falls as normal, or more rapidly, from high water until the turbines open at mid-tide after which the rate of fall declines or is halted. This

has potential negative implications for birds, although this effect occurs at the same time as the flats above the barrage become exposed. Energy generation on the flood and ebb, dual mode, reduces considerably the changes in exposure of the intertidal area and so reduces potential impacts on the bird community. The implications for tidally feeding fish are the opposite to those of the birds with greater periods for foraging available due to the retention/raising of water levels. The economics of a barrage or fence scheme scale with the volume of the tidal prism and hence the most favored schemes tend to involve large estuaries or bays. For example one option proposed in the Severn Tidal Power feasibility study could see up to 520km² of the estuary impounded, compared with the 17 km² at La Rance and 6 km² at Annapolis Royal. Another UK scheme in the Mersey River would involve an impoundment of 61 km² but even this would be sufficient to generate changes in the tidal range at locations all around the Irish Sea. The larger the scheme the more likely that there will not be alternative feed sites nearby. In the UK the quantity and quality of the food on the feeding grounds of over-wintering waders is the parameter that determines survival to the next breeding season. Thus, reduced feeding areas, increased foraging costs (extra flights between sub-optimal grounds) or lower food quality will directly impact on population size [29].

Changed spatial flow patterns will result in altered patterns of sediment deposition and movement that will have impacts on benthic communities. The outflow will be constrained to a number of sites, where the turbines are, and in these areas sediments will be scoured and coarsened while upstream of the barrage the reduced flows and periods of no flow will lead to increased siltation and potentially an increasing quantity of fine material in the deposits. Changes in the nature of the habitats will alter their suitability as nursery or spawning areas for fish. Tidal fences are not expected to alter the timing or amplitude of the tides as shown in figure 2.9.

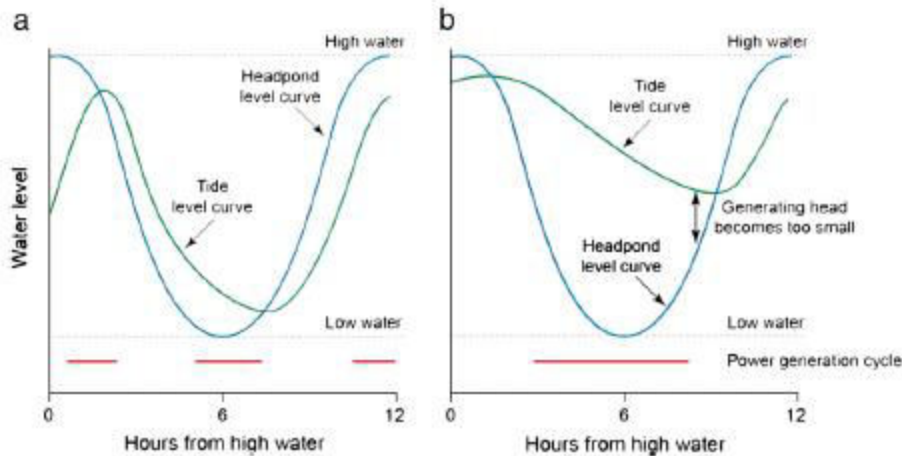


Fig. 2.9 The normal tidal curve and the modified tidal curve in the headpond above a tidal barrage in an estuary for (a) dual cycle generating and (b) ebb only generation.

3. Dynamic Tidal Power

Dynamic tidal power or DTP is a new and untested method of tidal power generation. It would involve creating large dam-like structure extending from the coast straight to the ocean, with a perpendicular barrier at the far end, forming a large 'T' shape. This long T-dam would interfere with coast-parallel oscillating tidal waves which run along the coasts of continental shelves, containing powerful hydraulic currents. Dynamic Tidal Power or DTP is the most complicated, least well understood tidal power scheme yet conceived [30]. Basically, dynamic tidal power make use of the fact that ocean tides don't operate strictly perpendicular to the shore, but also flow in parallel to the shore as well. This feature of tides would allow a type of barrage to be built perpendicular to the shore to harvest energy from the tides as they flow parallel to the shore as the diagrams in figure 2.9.1 (a) and figure 2.9.1 (b) below illustrate.

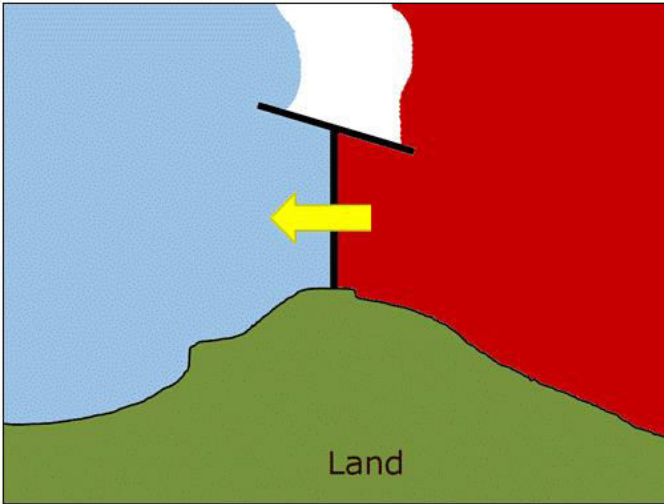


Figure 2.9.1 (a) the right angle to oceans tides

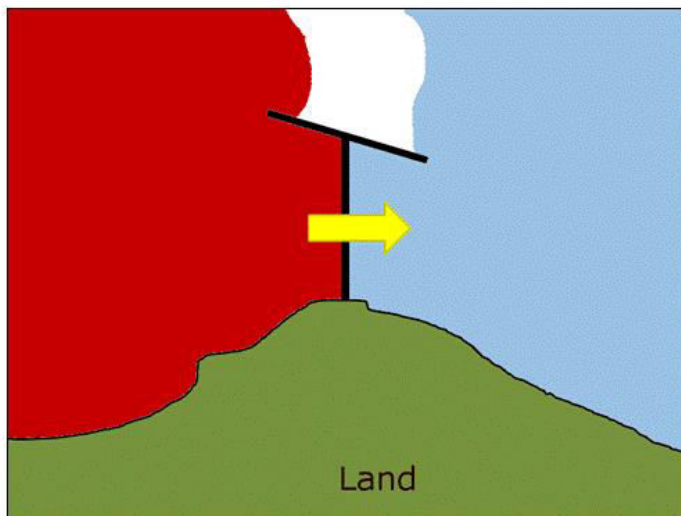


Figure 2.9.1 (b) the left angle to oceans tides

In the diagrams above, red represents relative high water and blue represents relative low water. The heights are relative to the barrage that is shown in black and which looks like a large “T.” The concept is based on the fact that tides flowing in one direction will tend to build up behind a barrier, like the barrage, and so create a height difference that can be used to generate power. When the tide shifts direction, something that happens every 12 hours, the height difference shifts sides. The system only works if the barrage is at least 30 kilometers long and only if the turbines work in both directions. So far, the system is 100% theory and has never been put to the

test. The science and math are sound, but without experiment there is no way to be certain the scheme will really work [31].

Advantages of Dynamic Tidal Power over Other Forms of Tidal generation

The main advantage of dynamic tidal power is that a single installation could produce anywhere from 8 to 15 gigawatts of power, orders of magnitude more than any other tidal energy system. An 8 GW installation could generate over 20 terawatt-hours of electricity in a year, which is enough for more than three million Europeans. The second advantage to DTP is that it is stable. Because it generates power no matter which direction the tide is moving, the system is more continuous than other forms of tidal energy. It is more reliable than any other renewable like solar or wind because the tides are constant, predictable, and not influenced by cloud, lack of wind, drought, etc [31]. Dynamic tidal power doesn't require a high head. In other words, water levels need not be dramatically higher on one side of the barrage compared to the other to generate the large amounts of power anticipated. This means that many more locations are suitable for DTP than for tidal barrage or tidal stream generators.

Finally, DTP offers the potential for combined function such as port protection, integration with wind turbines, aquaculture and research facilities, and more.

Challenges of Dynamic Tidal Power

A major challenge is that a demonstration project would yield almost no power, even at a dam length of 1km or so, because the power generation capacity increases as the square of the dam length (both head and volume increase in a more or less linear manner for increased dam length, resulting in a quadratic increase in power generation). Economic viability is estimated to be reached for dam lengths of about 30 km. Other concerns include: shipping routes, marine ecology, sediments, and storm surges. Amidst the great number of challenges and few environmental impacts the method of utilizing tidal power to generate electricity has great potential and is certainly a technology most of the countries will try to harness in near future [33].

2.6 ADVANTAGES AND DISADVANTAGES OF OCEAN TIDAL POWER

Tidal power is yet to attract significant renewable energy investment, even despite having good potential in many areas around the world. This is as a result of the advantages and disadvantages of tidal power.

Advantages: Tidal power belongs to renewable energy sources meaning it cannot be depleted like fossil fuels can. Tidal forces have their origin in the gravitational interaction with the Moon and Sun, meaning that we could harness tidal power as long as Moon and Sun continue to exist. The efficiency of tidal power. Tidal power belongs to the most efficient energy sources by having efficiency of approximately 80%, this is much better efficiency as compared to other more popular renewable energy sources such as solar and wind. Tides are predictable, and this predictability is also one of the advantages that tidal power has over other energy sources because rise and fall of tides are much more cyclic than random weather patterns. This predictability gives us knowledge when the tides will be in and out. Harnessing tidal power has positive impact on climate change because it produces no greenhouse gas emissions. Harnessing tidal power on larger scale could even lead to reduced import of foreign fuels and improve our energy security because we wouldn't have to rely so much on expensive foreign fuel import to satisfy our growing energy demand. Barrages and small dams used to harness tidal power could protect coastal areas or ship ports from dangerous tides during a stormy weather [32]. Ocean tides are shown in figure 2.9.2.



Fig. 2.9.2 Ocean tides

Disadvantages:

Environmental effects of tidal power generation are similar in many ways to those of wave power and offshore wind power generation. Assessments have identified a number of potential environmental impacts from tidal energy development. There are a number of indirect ecological effects that would result from extensive installation of offshore renewable energy developments.

These include:

- Alteration of currents and waves;
- Alteration of substrates, sediment transport and deposition;
- Alteration of habitats for benthic organisms;
- Noise during construction and operation;
- Emission of electromagnetic fields;
- Toxicity of paints, lubricants, and antifouling coatings;
- Interference with animal movements and migrations; and
- Strike by rotor blades or other moving parts.

High cost per kilowatt hour of energy output. The typical domestic retail electricity rate in Nova Scotia is \$138 / MWh, while the tidal stream feed-in tariff in Nova Scotia is \$652 / MWh – 5 times the current rate. In its Environmental Assessment (EA) of the ORPC in-stream tidal project in Cobscook Bay, Maine (FERC Project No. 12711-005), FERC estimates the cost of power to be \$1,062.25 / MWh, while FERC estimates the cost of power from the Admiralty Inlet Tidal Project (FERC Project No. 12690-005) in Washington State to be \$8,552.27 / MWh. The low energy density of tidal stream devices requires the deployment of either massive machines or multiple arrays of machines covering the proximate sea floor at various depths in order to generate a modest amount of energy.

2.7 TIDAL POWER LOCATIONS

Tidal Wave Energy is still a very niche technology with tidal barrages generating most of the electricity in a few power stations. Most of the tidal power plants using the modern tidal turbine technology are still in the pilot phase and generate negligible power. However tidal power

stations have the potential to generate large amounts of energy in a non-polluting way. Though Tidal Technology is still in the baby phase, a number of companies are engaged in research in Tidal Technology and a large number of Tidal Stations are being built in Europe and USA. Here are a list of major Tidal Power Plants in the world. Expect this list to grow much bigger in the future as human interest in undersea technology grows as resources on land become fewer and more expensive.

- Rance Tidal Power Plant is the world's first and the most famous Tidal Power Plant in the world. The 240 MW power plant is located on Rance River, Brittany, France and was started almost 45 years ago. The Tidal Power Station is run by French state owned electricity giant EDF .
- Annapolis Royal Tidal Power Plant is North America's only power station and is located in Nova Scotia, Canada with a 20 MW power capacity. This Tidal Power Plant is built on the Bay of Fundy was built in 1984. The power plant operates on the same principle of tidal barrage and it has also faced issues of damage to river and marine life.
- Jiangxia Tidal Power Plant is China's only Tidal Power Station and has a capacity of 3.2 MW. It is located in Zhejiang, China.
- Kislaya Guba Tidal Power Plant is a pilot plant built in Russia with a capacity of 1.7 MW . The plant was completed recently in 2004 though construction was started way back in 1968.
- Strangford Narrows SeaGen Tidal Power Plant is the first large scale Tidal Power Station which has been built using Tidal Turbine Technology. The Tidal Power Plant is located in Northern Ireland. This is a pilot plant built by Marine Current Turbines and it started in 1994 with a small 15 Kilowatt Tidal Turbine.
- Uldolmok Tidal Power Plant is Asia's 2nd largest Tidal Power Plant with a capacity of 1 MW. The South Korean plans to expand the capacity to 90 MW by 2013 and is located in Jindo County of South Korea. Note the South Korean government is the most aggressive government in building out Tidal Wave Energy Power Plants.
- Aguçadoura Wave Farm in Portugal is the world's first wave farm with a capacity of 2.25 MW. This Tidal Power Plant uses Pelamis Wave Energy Converters . The plant was

supposed to be expanded to 21 MW before one of the promoters of this tidal power station Babcock and Brown went bankrupt [34].

Future Tidal Wave Plants

- Incheon Tidal Wave Power Plant will be the biggest plant in the world when it is built. The Power Plant in Incheon, South Korea will have a capacity of 1320 MW with 44 Turbines of 30 MW power capacity. The cost of the power plant will be around \$3.4 billion and has a planned completion date of 2017.
- Sihwa Lake Tidal Power Plant unlike other Power Plants is already being constructed and with a capacity of 254 MW will be the biggest Tidal Power Plant in the world when completed. The plant is located in South Korea. The cost of the plant is estimated to be between \$300-400 million which compares quite favorably with other forms of energy.
- Garorim Bay Tidal Power Plant like the above 2 plants is also to be located in South Korea and is being built by Korea Western Power Company. The capacity of the plant will be 520 MW
- Penzhin Tidal Power Plant is proposed to be built in Russia. This power plant will be the largest power plant in the world if it is ever built with a gargantuan power capacity of 87000 MW. The Tidal Power Station will be built on Penzhin Bay on the border of Magadan Oblast.
- Gulf of Kutch, Gujarat Tidal Power Plant – India does not have a Tidal Power Plant till now, however the western state of Gujarat is strongly pushing for building a power plant in the Gulf of Cambay. The Tidal Energy Plant will use the same principle used in Tidal Barrages.
- Dalupiri Blue Energy, Philippines is like the Russian Power Plant still on the drawing stage and looks highly unlikely that it will be built. This Tidal Power Plant also has an ambitious capacity target of above 2 GW.

- Cornwall Wave Hub is being planned with a first phase of 20 MW power capacity. This Tidal Power Plant will use Tidal Turbines and the second phase will lead to another 20 MW of capacity leading to 40 MW of overall electricity capacity.
- Ocean Power is planning to build a small 150 kW Tidal Power Plant off Oregon in the United States. [35]

Figure 2.9.3 shows favorable tidal power plant locations in the world. The speed of the ocean tides is on the average 10 m/s.



Fig2.9.3. Locations with the most potential for tidal energy [35]

2.8 ENVIRONMENTAL EFFECT OF TIDAL POWER GENERATION

Environmental effects of tidal power generation are similar in many ways to those of wave power and offshore wind power generation. Assessments have identified a number of potential environmental impacts from tidal energy development. Gill (2005) [36] describes a number of

indirect ecological effects that would result from extensive installation of offshore renewable energy developments. These include:

- Alteration of currents and waves;
- Alteration of substrates, sediment transport and deposition;
- Alteration of habitats for benthic organisms;
- Noise during construction and operation;
- Emission of electromagnetic fields;
- Toxicity of paints, lubricants, and antifouling coatings;
- Interference with animal movements and migrations; and
- Strike by rotor blades or other moving parts.

Effects on biological resources could include alteration of the behavior of animals, damage and mortality to individual plants and animals, and potentially larger, longer-term changes to plant and animal populations and communities. Development of tidal energy involves technology testing, site characterization, device installation, operation and maintenance, and decommissioning. Many installation and decommissioning effects have close analogues to existing industries (e.g., offshore wind) and are short-term. Consequently, this report places an emphasis on operational effects experienced over the long term and installation/decommissioning effects unique to tidal energy.

Installation Effects

Installation of tidal power generation devices may cause significant disturbance to the local environment. However, other than the actual placement of persistent structures (i.e., the device and power cables), most installation effects are likely to be temporary (weeks to months, with some effects lasting longer). Stressors present during deployment are similar to those from other construction activities in the marine environment [37] and include construction noise (i.e., air compressors), increased vessel activity, and habitat disturbance associated with installation of anchors and power cables. The area of disturbed habitat depends on the number of devices to be installed and type of foundation. If project installation involves pile driving, nearby noise levels are likely to exceed damage threshold values for fish and marine mammals [38], potentially causing temporary or lasting harm to affected individuals or populations. Deployment timing

may help to mitigate the effects of these stressors on marine organisms, especially migratory fish, marine mammals, and seabirds.

2.9 THE ECONOMICS OF TIDAL POWER

Benefits

Investment in tidal generation adds to the generation capacity on the system and can thus defer investment in other forms of generation. This is a benefit of tidal generation and is measured by the capacity credit. The capacity credit of a generator can be considered as a measure of the amount of conventional generation that could be displaced by the renewable production without making the system any less reliable. The capacity credit for tidal stream generation on the Irish system was estimated in [39], and for a turbine of 336MW it is estimated at approximately 18%. In other words, an investment of 100MW in tidal generation will displace the need for investment in 18MW of conventional generation. Based on current building costs for a combined cycle gas turbine, this results in a benefit of approximately €9 million per annum, or €27000 per MW of tidal installed [40]. Another benefit of tidal generation is a reduction in harmful emissions as tidal generation is likely to displace the output of some thermal units. For the Irish electricity system, emissions benefits have been estimated at €16million per annum, assuming a price of €30 per ton of CO₂, €150 per ton of SO₂ and €3,000 per ton of NO_x. This equates to approximately €48k per MW installed of tidal [40]. In addition, a reduction in the operation of thermal units can also lead to a fuel cost saving as tidal generation, with a zero fuel cost, replaces units with significant fuel costs. The fuel savings from tidal generation were estimated to be approximately €39 million per annum, or €116000 per MW installed [40].

Costs

The predictable nature of the tidal output is an advantage compared to other renewable. The output of renewables such as wind, wave and solar is relatively unpredictable thus power system operators must carry additional reserve capacity to protect against periods of overestimated output [41]. This is a system cost imposed by these other renewable. However, additional backup

reserve capacity is not required for tidal generation due to its predictable nature. In the day to day operation of electricity systems, conventional generation units are required to cycle in order to meet the demand. This cycling includes ramping up and down and turning on and off. When a unit is cycled, the boiler, steam lines, turbine and auxiliary components undergo large thermal and pressure stresses which result in damage [42]. This damage accumulates over time and eventually leads to accelerated component failures and forced outages. The costs associated with cycling include additional operation and maintenance spending associated with increased overhauls, higher heat rates due to low load and variable operation, auxiliary power, fuel during start up, unit life shortening, increased operator error due to greater hands-on operation, etc. It is estimated that these costs can range from €200 to €500,000 (including fuel cost) per single on-off cycle depending on the type of unit [43]. The tidal generation has four peaks and troughs per day representing the tidal current coming in and out twice a day. This fluctuation is particularly apparent during a spring tide when the variations are at their maximum. Thus, although the tidal generation is predictable its variability causes a challenge for system operators. It was found in [44] that as tidal penetration increases, the number of starts on the system increases. This is due to the magnitude of the variations in tidal output increasing as the installed tidal generation increases. The cost of this additional cycling activity as a result of the increased tidal generation was calculated for each of the units on the system and is estimated at up to €23m per annum. There have been no comprehensive network reinforcement studies completed for Ireland with respect to tidal generation. However, experience at the test sites has highlighted significant technical issues with laying network cables over the undulating sea-beds found at attractive resource sites. This issue may in fact limit the number of feasible sites to less than that estimated.

Break-even Capital Costs

The previous sections discussed the benefits and some costs associated with increases in tidal generation. These estimate total benefits of €64m per annum and cycling costs of €23m. However, capital, operation and network costs have yet to be considered. Since tidal generation is still in its infancy clearly defined capital costs have not yet been established and forecasting the likely capital costs in the future could be erroneous. Thus, rather than attempting to quantify the total net benefits of tidal generation [44] determines the maximum amount that the combined

capital, operation, maintenance and network costs can be to ensure positive net benefits for tidal generation. Using the estimates detailed in the previous two sections, €41m (€64m - €23m) is the maximum that these combined costs can be to ensure positive net benefits for 336MW of tidal generation. Putting this amount into perspective, if it is assumed that the operation and maintenance costs of tidal generation were equal to €60,000 per MW installed per annum, annual O&M cost for 336MW of tidal generation would be €20m. While this figure may initially appear to be high, O&M cost of €60,000/MW installed per annum are in fact less than those of an offshore wind turbine. Given that the moving parts of the tidal turbines operate below the water line, they are likely to incur greater damage to parts compared to a wind turbine with moving parts above the water line. In general O&M costs for offshore energy tend to be high given accessibility issues and greater infrastructure costs than onshore developments.

If it were assumed that no network reinforcement was required with 336MW of tidal, then the capital costs would have to be less than €21m per annum to ensure positive net benefits (€41m - €20m). If this is the annual cost of capital, then the total capital cost of 336MW of tidal would be approximately €180m (assuming an interest rate of 8% and a term of 15 years). This represents a capital cost of approximately €530,000 per MW installed of tidal generation. In other words, to ensure 336MW of tidal generation breaks-even the capital cost would have to be less than €530,000 per MW installed. The cheapest plant currently available on the Irish system is a peaking unit with a capital cost of €700,000/MW installed [45]. Thus, the benefits of tidal generation are such that the capital costs would have to be dramatically lower than the cheapest conventional unit in order to be economically viable from a societal perspective. Thus, it is not unreasonable to conclude that, given the current conventional plant mix, tidal generation will produce negative net benefits.

CHAPTER THREE

3.0 MODELING AND SIMULATION OF 6 MW DFIG TIDAL TURBINE SYSTEM FOR DIFFERENT FAULT CONDITIONS

In this chapter MATLAB/ SIMULINK is used to model a 6 MW tidal power site. The tidal energy system consists of four 1.5 MW tidal turbines connected to a 25 kV distribution system. The power generated is transmitted to a 120 kV grid through a 15 km, 25 kV feeder. The designed system consists of a 2 MVA plant consisting of a 1.68 MW induction motor load along with a 200 kW resistive load. The dynamic behavior of the system is analyzed by simulation of different fault conditions in the system.

3.1.1 Description of the tidal Generation System

A 6 MW tidal power generation having four, 1.5 MW tidal turbines connected to a 25 kV distribution system ensures power to a 120 kV grid through a 30 km, 25 kV feeder line. A 2300V, 2 MVA plant with a motor load (1.68 MW induction motor at 0.93 pf) and of a 200 kW resistive load is linked onto the same feeder. Both tidal turbine and motor load have protection systems for monitoring voltage, current and machine speed. DFIG DC link voltage is also monitored. Tidal turbines use an induction generator having a wound rotor and an AC/DC/AC IGBT based PWM converter. The stator winding is linked directly to the 50 Hz grid and the rotor is fed at variable frequency through the AC/DC/AC converter. DFIG technology enables extraction of maximum energy from the tides for low tidal speeds through optimization of turbine speed, while lowering turbine mechanical stresses during heavy tides. The turbines optimum speed to produce maximum mechanical energy for a given tidal speed is directly proportional to tidal speed. The rotor runs at sub synchronous speed for tidal speeds lower than 10 m/s and at super synchronous speeds for higher tidal speeds. The graph of turbine output power against the turbine's speed is shown in Figure 3.1.0 for tidal speeds ranging from 5 m/s to 16.2 m/s. The DFIG is controlled so that it follows the red curve. The turbine speed optimization is between point B and point C on this curve. An additional advantage of DFIG technology is its ability to generate or absorb reactive power through power electronic converters thereby

eliminating the need for capacitor banks as in squirrel cage induction generators (www.mathworks.com). The SIMULINK model of the 6 MW power generation is shown in Figure 3.1.1.

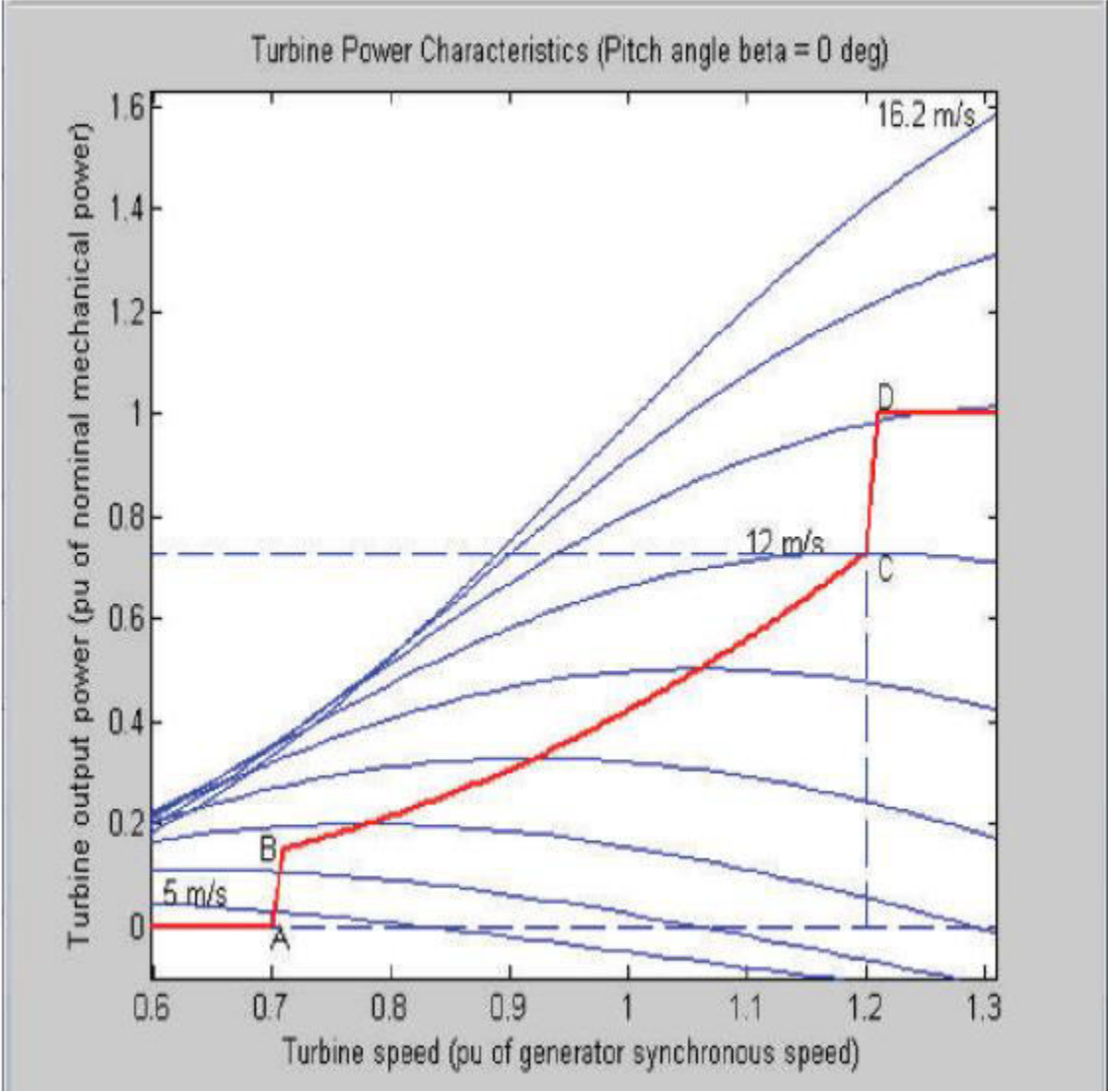


Figure 3.1.0 Mechanical Characteristics of Turbine

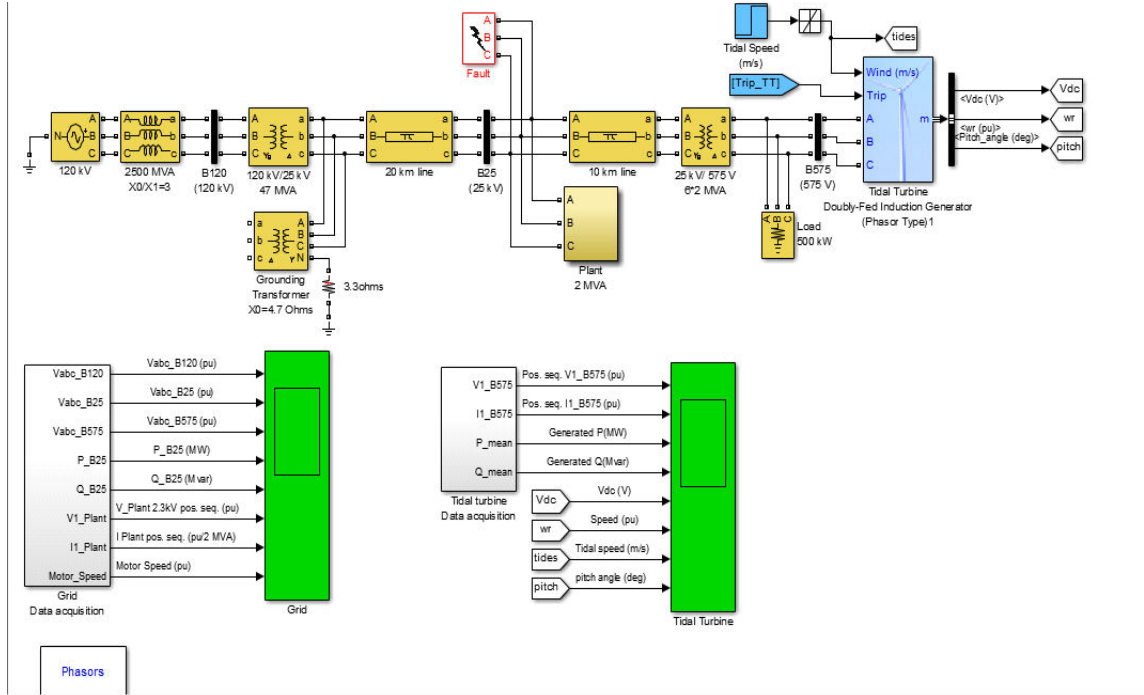


Figure 3.1.1 SIMULINK Model of 6 MW Tidal Power System

3.1.2 Tidal Turbine Modeling

The steady state power characteristic of the tidal turbine is the basis of this model. The drive train's stiffness is infinite and both friction factor and turbine inertia should be combined with the generator. The output power of the tidal turbine is given by the following equation.

$$P_m = \left(\frac{1}{2}\right)C_p(\lambda, \beta)\rho Av^3 \quad (19)$$

Where, the above equation can be normalized. In the pu system we have

$$P_m(pu) = k_p c_p - pu v - pu^3 \quad (20)$$

A generic equation is used to model $c_p(\lambda, \beta)$.

$$c_p(\lambda, \beta) = C_1 \left(\frac{C_2}{\lambda_i} - C_3 \beta - C_4\right) e^{-C_5/\lambda_i} + C_6 \lambda \quad (21)$$

Where

$$\frac{1}{\lambda_i} = \frac{1}{\lambda + 0.08\beta} - \frac{0.035}{\beta^3 + 1} \quad (22)$$

The coefficients C_1 to C_6 are;

$$C_1=0.5176$$

$$C_2=116$$

$$C_3=0.4$$

$$C_4= 5$$

$$C_5= 21$$

$$C_6=0.0068$$

The C_p - λ characteristics, for different values of the pitch angle β , are illustrated in Figure 3.1.2. The maximum value of C_p ($C_{pmax}= 0.48$) is achieved for $\beta = 0$ degree and for $\lambda = 8.1$.

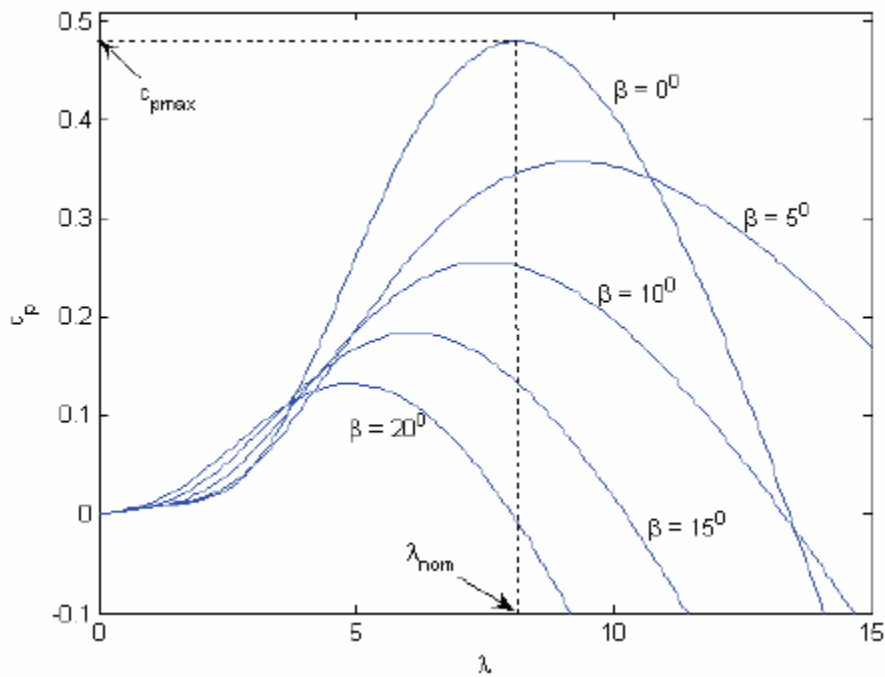


Figure 3.1.2 Power Coefficient vs. λ Characteristics

Figure 3.1.3 illustrates the SIMULINK tidal turbine model. The three inputs are the generator speed in pu, pitch angle β , in degrees and tidal speed in m/s. The output is the generator shaft's torque.

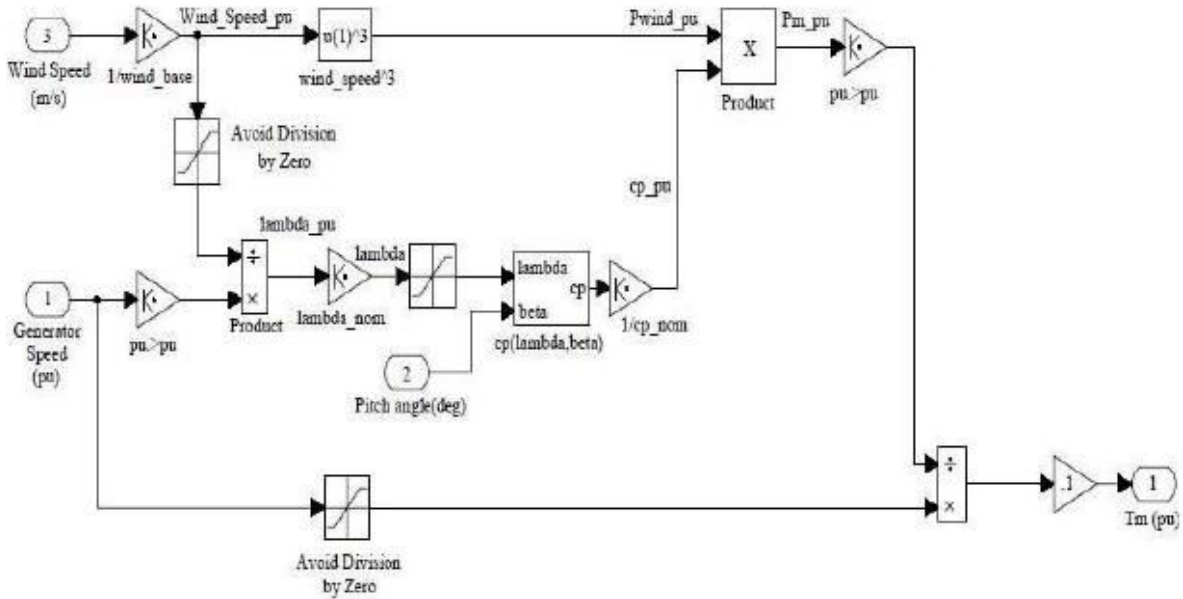


Figure 3.1.3 SIMULINK Model of Tidal Turbine

3.1.3 Modeling of DFIG

The DFIG is represented by a fourth order state space model and a second order system represents the mechanical part. All electrical variables and parameters are referred to the stator. All stator and rotor quantities are in a two axis reference frame (d q frame). The Table 3.1 defines the subscripts used in the model (The Math Works, "Sim Power Systems for Use with SIMULINK", User's Guide Version 4).

Table 3.1 Definition of Subscripts

Subscript	Definition
d	Direct axis
q	Quadrature axis
r	Rotor
l	Leakage Inductance
s	Stator quantity
m	Magnetizing inductance

The d and q axis equivalent circuit of the machine is shown in Figure 3.1.4.

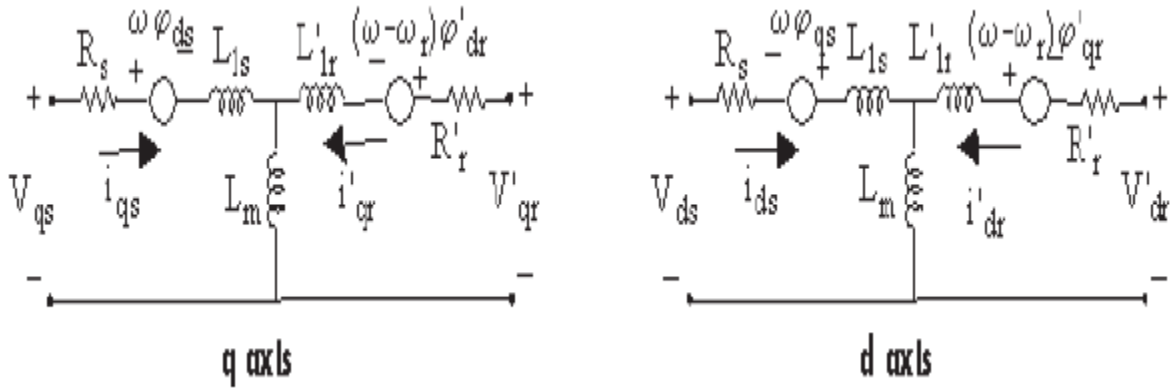


Figure 3.1.4 d q Axis Equivalent Circuit of DFIG

In the above figure m is the reference frame angular velocity and m_r is the electrical angular velocity. The equations governing the dynamics of the machine are given below.

$$V_{qs} = R_s i_{qs} + \frac{d\phi_{qs}}{dt} + \omega \phi_{ds} \quad (23)$$

$$V_{ds} = R_s i_{ds} + \frac{d\phi_{ds}}{dt} + \omega \phi_{qs} \quad (24)$$

$$V'_{qr} = R'_r i'_{qr} + \frac{d\phi'_{qr}}{dt} + (\omega - \omega_r) \phi'_{dr} \quad (25)$$

$$V'_{dr} = R'_r i'_{dr} + \frac{d\phi'_{dr}}{dt} + (\omega - \omega_r) \phi'_{qr} \quad (26)$$

$$\varphi_{qs} = L_s i_{qs} + L_s i'_{qr} \quad (27)$$

$$\varphi_{ds} = L_s i_{ds} + L_m i'_{dr} \quad (28)$$

$$\varphi'_{qr} = L'_r i'_{qr} + L_m i_{qs} \quad (29)$$

$$\varphi'_{dr} = L'_r i'_{dr} + L_m i_{ds} \quad (30)$$

$$T_e = 1.5p(\varphi_{ds} i_{qs} - \varphi_{qs} i_{ds}) \quad (31)$$

$$L_s = L_{1s} + L_m \quad (32)$$

$$L'_r = L'_{1r} + L_m \quad (33)$$

The dynamics of the mechanical system is governed by the following equations;

$$\frac{d}{dt} \omega_m = \frac{1}{2H} (T_e - F\omega_m - T_m) \quad (34)$$

$$\frac{d}{dt} \theta_m = \omega_m \quad (35)$$

The definitions of the parameters in the model are defined in Table 3.2

Table 3.2 Definition of Parameters in the Model

Rs, Lls	Stator resistance and leakage inductance
Lm	Magnetizing Inductance

L_s	Total stator inductance
V_{qs}, i_{qs}	q axis stator voltage and current
V_{ds}, i_{ds}	D axis stator voltage and current
Φ_{qs}, Φ_{ds}	Stator q and d axis fluxes
Θ_m	Rotor angular position
P	Number of pole pairs
Ω_r	Electrical angular velocity ($\omega_m \times p$)
Ω_m	Angular velocity of the rotor
Θ_r	Electrical rotor angular position ($\Theta_m \times p$)
T_e	Electromagnetic torque
T_m	Shaft mechanical torque
J	Combined rotor and load inertia coefficient. Set to infinite to stimulate locked rotor.
H	Combined rotor and load inertia constant. Set to infinite to stimulate locked rotor.
F	Combined rotor and load viscous friction coefficient
L'_r	Total rotor inductance
R'_r, L'_{lr}	Rotor resistance and leakage inductance
V'_{qr}, i'_{qr}	q axis rotor voltage and current
V'_{dr}, i'_{dr}	d axis rotor voltage and current
Φ'_{qr}, Φ'_{dr}	Rotor and d axis fluxes

3.1.4 Back to Back AC/DC/AC Converter Modeling

The converter system's mathematical modeling is realized by using various types of models, which are divided into two: Mathematical functional models and mathematical physical models based on equation or graphic. The functional model reveals the relationship between the system's input and output signal in the form of mathematical function (s) and hence the system's primary elements are not modeled separately. Simplicity and quick time domain simulation are this modeling's advantages and the penalty is of losing accuracy. This was a popular approach in connection with DFIG modeling, where simulation of converters was undertaken based on expected controller response and not actual power electronics devices modeling. It is assumed that converters are ideal and DC link voltage between them stable. Hence based on converter control, a controllable voltage (current) source can be implemented and represent operation of the converter model's on the rotor side as shown in figure 3.1.5. In this research, a graphic oriented switch by switch representation of back to back PWM converters and modulators for rotor and stator side converters, is used where IGBT and reverse diode devices are represented as a two state resistive switch which can take on two values like RON (close to zero) and ROFF (very high).

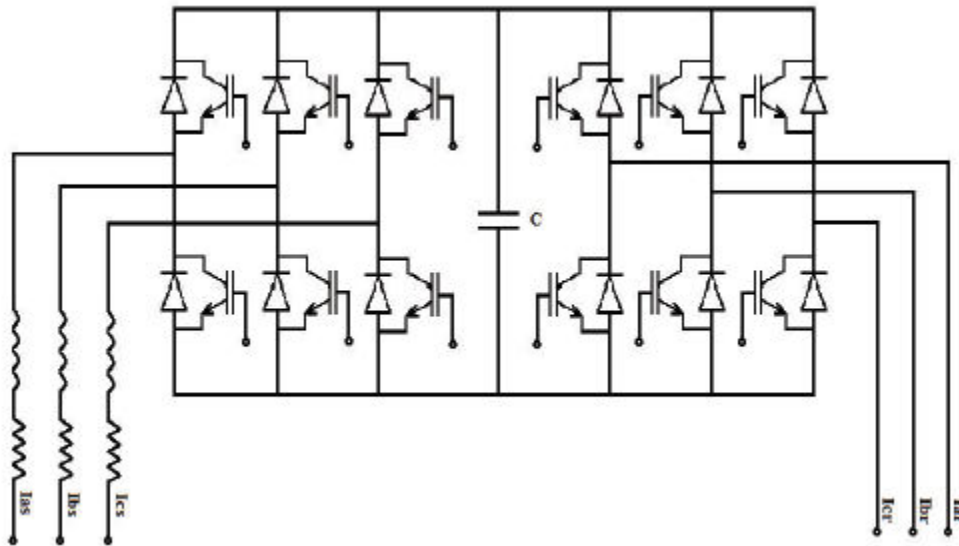


Figure 3.1.5 Back to Back AC/ DC/ AC Converter

3.1.5 Rotor Side Converter Control System

The tidal turbine connected to a DFIG. The AC/DC/AC converter has two parts; Rotor Side Converter and Grid Side Converter implemented through use of IGBT's to synthesize required

AC voltage from a DC source. The DC source is realized through a capacitor connected to the DC side. The Rotor Side Converter controls the tidal turbine output power. This control is shown in Figure 3.1.6 as the figure reveals, the actual power output measured at the turbine's grid terminals is summed with mechanical and electrical power loss and is compared with reference power obtained from tracking characteristic. The power regulator which is a PI controller reduces power error to zero. The regulator's output is the reference rotor current I_{qr_ref} that must be injected in the rotor by rotor converter. This produces the electromagnetic torque T_m . The AC voltage regulator compares the measured voltage with reference voltage and produces an output I_{dr_ref} . The current regulator takes the difference between I_{dr_ref} and I_{dr} and the difference between I_{qr_ref} and I_{qr} as inputs and produces an output V_r .

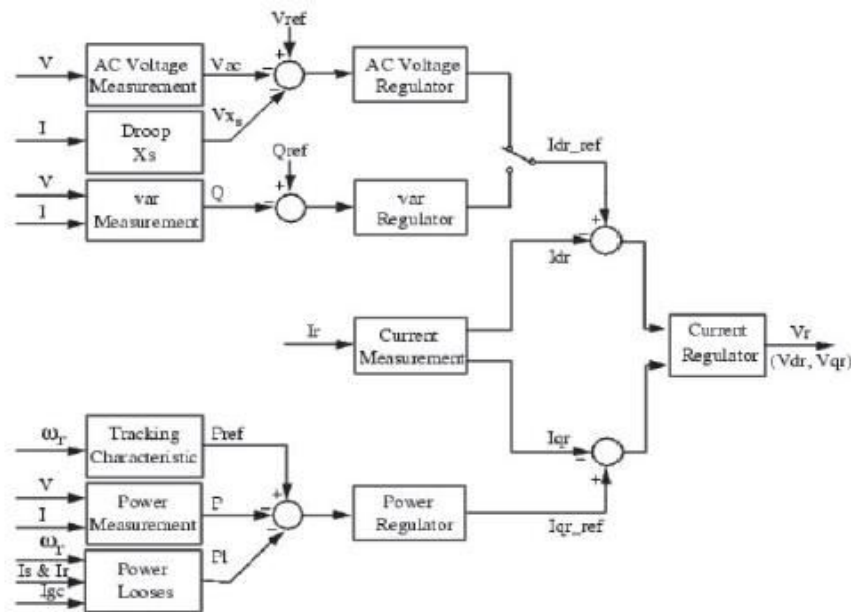


Figure 3.1.6 Rotor Side Converter Control System

3.1.6 Grid Side Converter Control System

The Grid Side Converter control system is shown in Figure 3.1.7. The voltage in the DC bus capacitor is regulated through use of converter C_{grid} which generates or absorbs reactive power. The outer regulation loop of the system includes the DC voltage regulator whose output is the reference current I_{dgc_ref} for the current regulator. The inner current regulation loop includes a

current regulator which controls magnitude and phase of the voltage V_{gc} generated from the I_{dgc_ref} produced by the DC voltage regulator and specified I_{q_ref} .

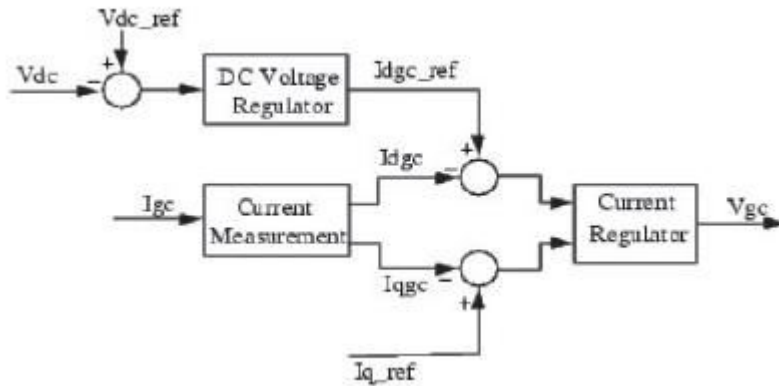


Figure 3.1.7 Grid Side Converter Control System

3.1.7 Tidal Turbine Protection Block

The Tidal turbine protection shown in Figure 3.1.8 provides protection for the tidal turbine where positive sequence voltage and current and DC voltage are provided as input and for their corresponding values trip data is used to check whether tripping should be permitted. Different reasons for tripping could be AC over voltage, under voltage, over current, under current, DC over voltage, over speed or under speed.

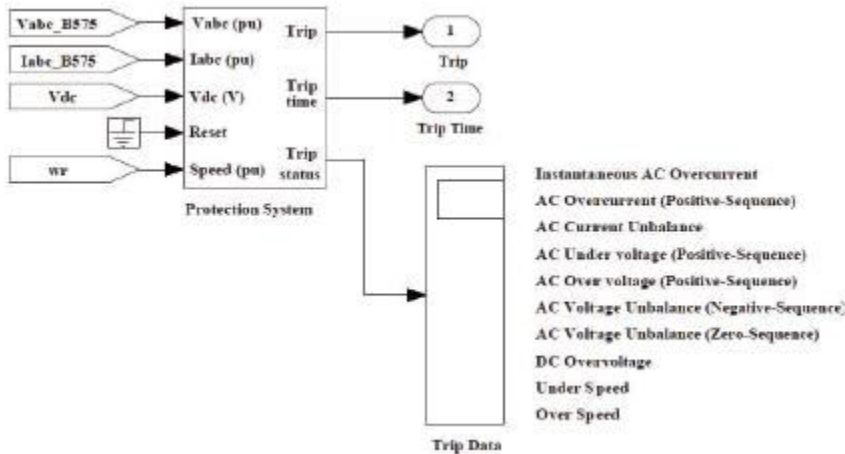


Figure 3.1.8 Tidal Turbine Protection Block

3.1.8 Tidal Turbine Data Acquisition System

The block diagram for generator data acquisition is shown in Figure 3.1.9 where the input signals are voltage and current which pass through gains and finally outputs that are provided are positive sequence current, voltage and active and reactive power mean values. Active and reactive power values calculated are as in per unit.

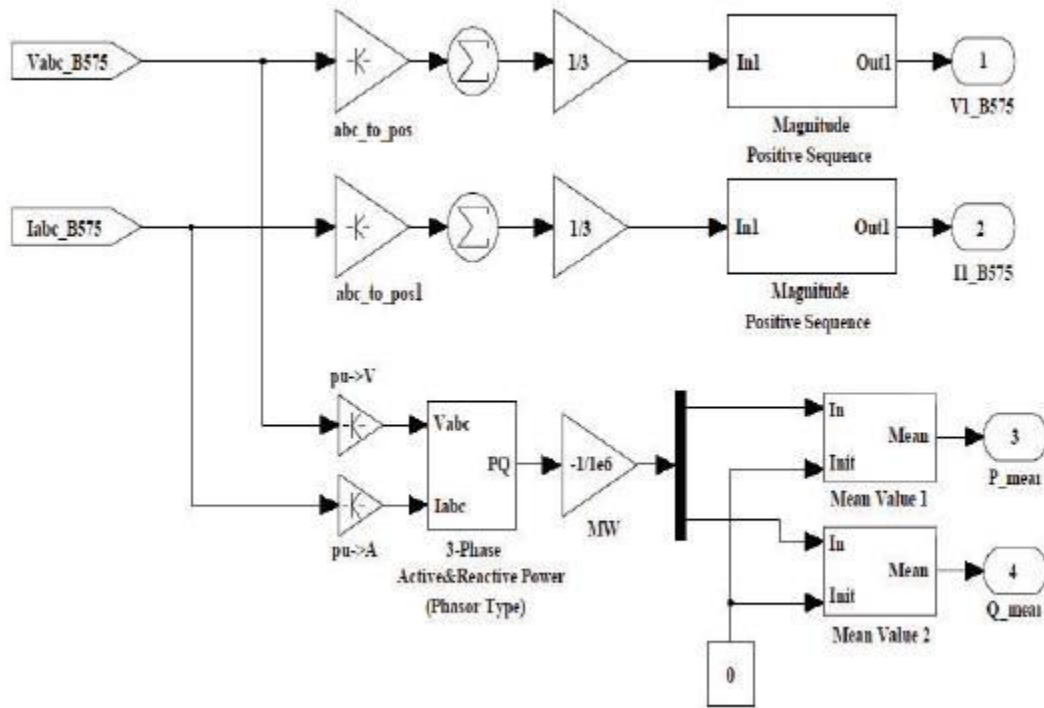


Figure 3.1.9 Tidal Turbine Data Acquisition System

3.1.9 Grid Data Acquisition

The block diagram for Grid data acquisition system is shown in Figure 3.2.0. The inputs are voltage, current, and speed to various blocks giving pu active and reactive power outputs along with motor speed. It utilizes sequence phase analyzer that outputs positive, negative, zero or all sequence components (magnitude and phase) of a three phasor set.

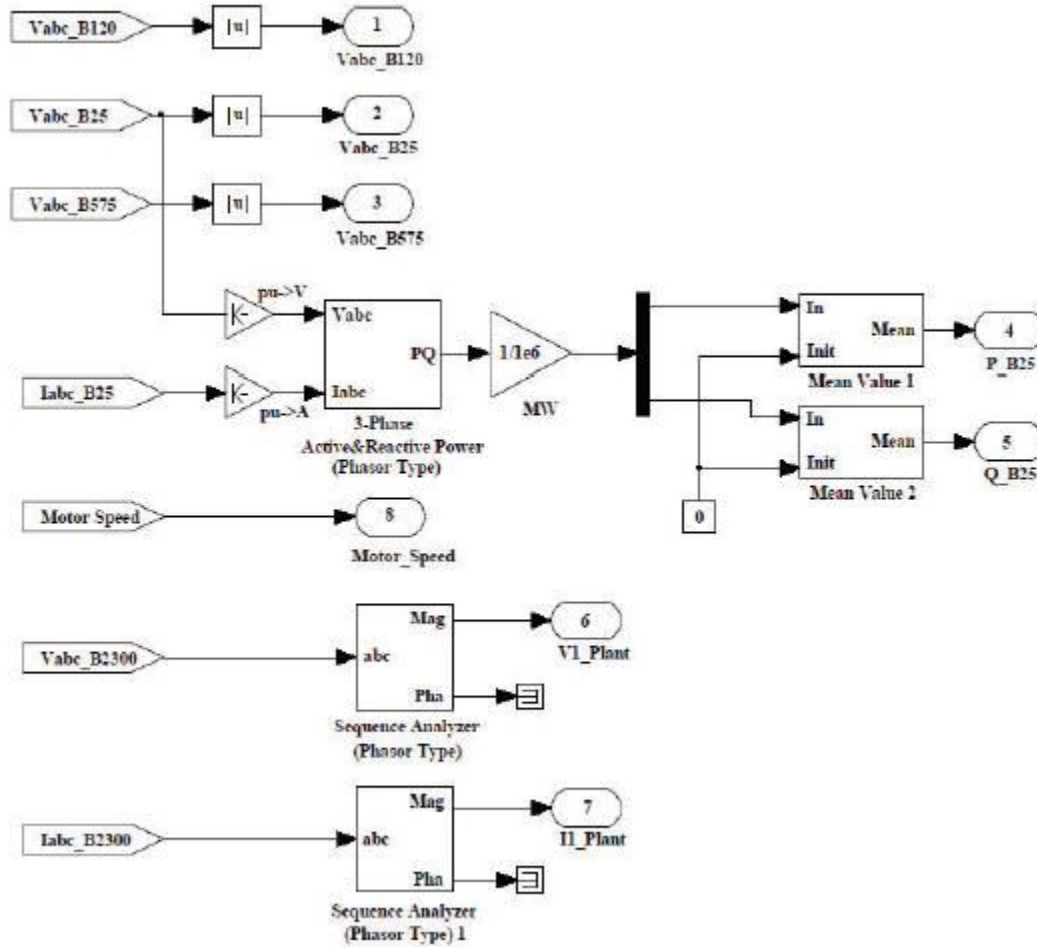


Figure 3.2.0 Grid Data Acquisition System

3.2.0 Simulation Results

The simulation of 6 MW tidal site is carried out for normal condition. Different types of faults were introduced on the 25 kV Line and the simulation results are presented in Figures 3.6 to 3.9. From the simulation results the following inferences can be made.

For normal condition, at a tidal speed of 13m/s

- i) The reactive power of the DFIG is controlled to maintain a grid voltage of 1 pu voltage as seen from Figure 3.2.1 (a). The figure shows that when the power output is connected to the site grid for power transmission, The grid voltage per unit is stable between 0.9996pu and 0.9997pu from Zero seconds to 100seconds.

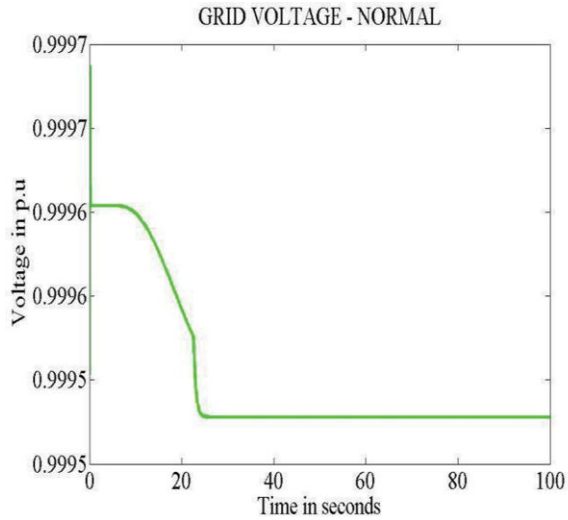


Figure 3.2.1 (a) Grid Voltage-Normal

- ii) The tidal site output voltage and the voltage in 25 kV line is also nearly 1 pu as seen from Figures 3.2.1 (b) and (c) respectively.

Figure 3.2.1 (b) shows that there is little variability of output voltage during normal condition which is with the range of 1 per unit.

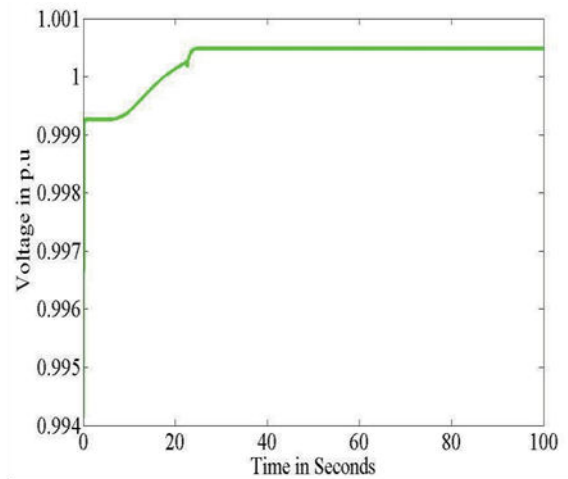


Figure 3.2.1 (b) The tidal site output voltage per unit.

Figure 3.2.1 (c) indicates that at normal conditions, the voltage per unit in the 25kV line is almost 1pu. Which ranges between 0.99425pu and 0.99475pu.

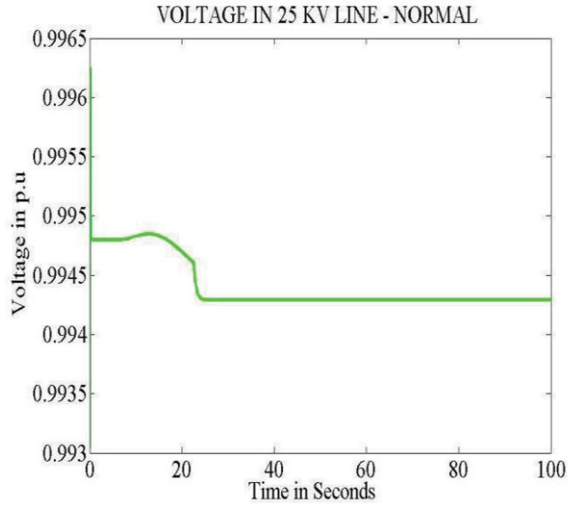


Figure 3.2.1 (c) Voltage In 25kV Line-Normal

- iii) The value of Vdc is nearly 1200V as seen from Figure 3.2.1 (d). The Direct Current Voltage of the tidal site varies between 1000V and 1200V after DC conversion.

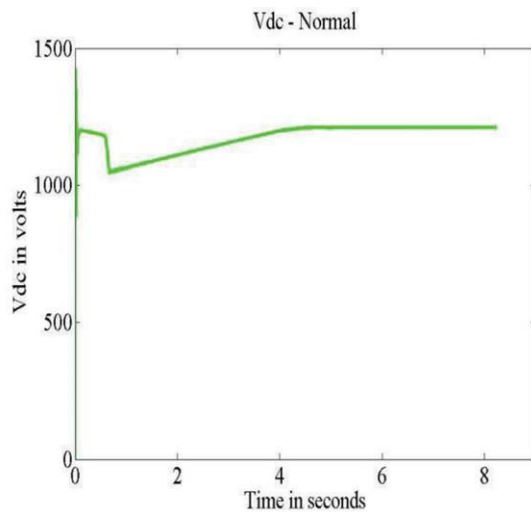


Figure 3.2.1 (d) Vdc-Normal

- iv) The real power generated by the tidal site is initially 1.2 MW and increases to a steady value of 5.5 MW as seen from Figure 3.2.1 (e). At t=10, the generated real power starts increasing smoothly together with the turbine speed to reach its rated value of 5.5MW in approximately 24 seconds.

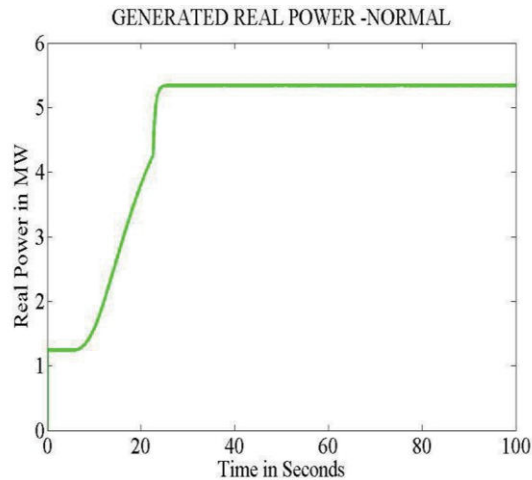


Figure 3.2.1 (e) Generated Real Power-Normal

- v) The reactive power of the tidal site is 0.22 MVAR initially and reduces to -0.15 MVAR as seen from Figure 3.2.1 (f). The figures shows that the generated reactive power at time zero, the tidal turbine absorbs 0.22 MVAR which generates downwards to -0.15 MVAR at time 20 seconds to control voltage at 1pu.

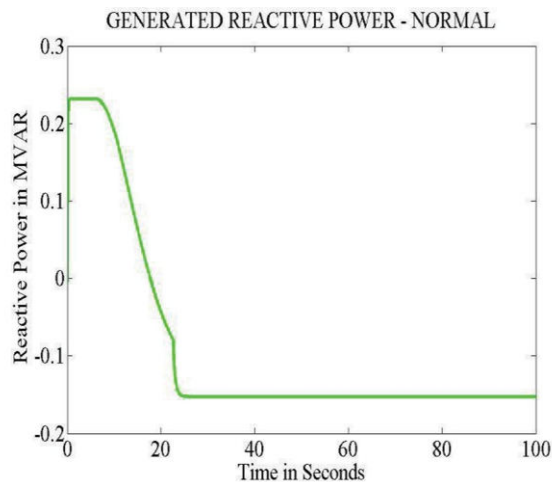


Figure 3.2.1 (f) Generated Reactive Power-Normal

- vi) The real power in the 25 kV line is initially 1.2 MW and reaches a steady value of -3 MW as seen from Figure 3.2.1 (g). At time zero the figure shows that the generated real power in 25kV line valued at 1.2MW. At time 10 seconds, the real power reduces gradually from 1.2 MW to a stable value of -3 MW.

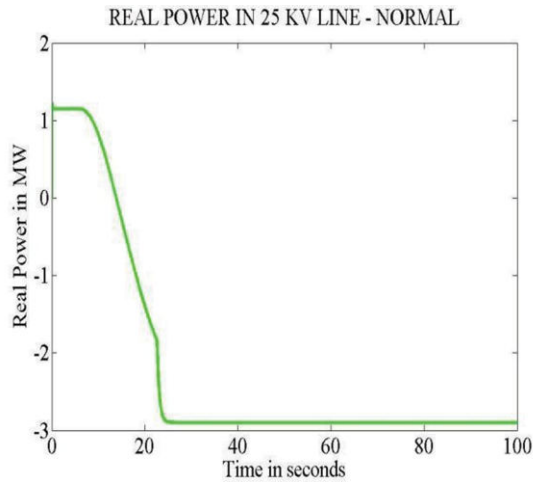


Figure 3.2.1 (g). Real Power In 25 KV Line-Normal

- vii) The reactive power in the 25 kV line is 0.4 MVAR and increases to a steady value of 1.1 MVAR as seen from Figure 3.2.1 (h).

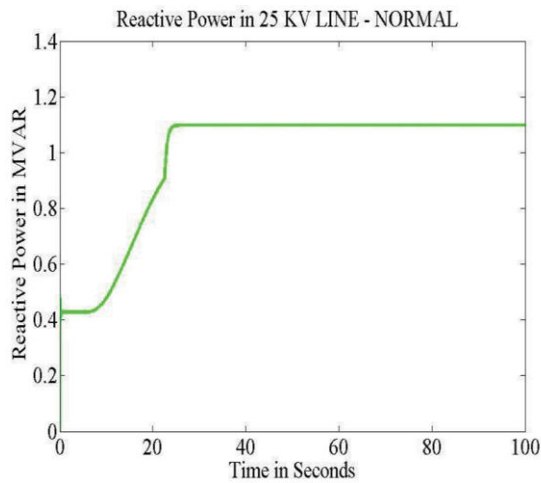


Figure 3.2.1 (h) Reactive Power in 25 kV Line-Normal

For a phase A to ground fault in the 25 kV line for $t = 5$ to 5.1 seconds

- i) During the fault, the Phase A voltage of the grid drops to 0.975 pu and phase C voltage of the grid drops to 0.983 pu and the phase B voltage of the grid is maintained at 1 pu as seen from Figure 3.2.2 (a).

Figure 3.2.2 (a) indicates that at time 5 seconds, phase A voltage of the grid side reduces steadily to 0.975pu (Red) at time 5.1 Seconds. While phase C voltage also drops to 0.983pu (Blue) at the same time. The Phase B voltage of the grid side remains steadily at 1pu (Green).

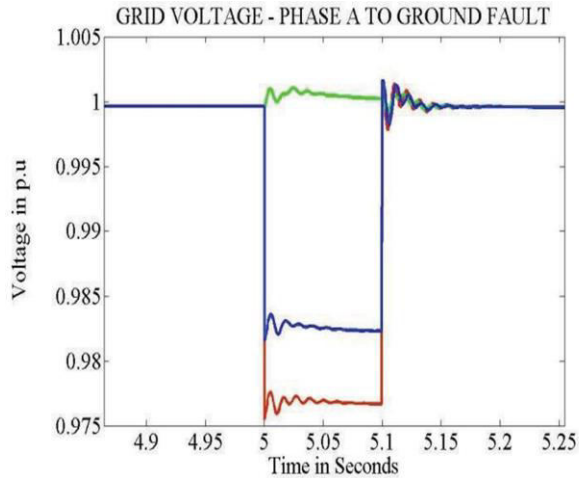


Figure 3.2.2 (a) Grid Voltage-Phase A to Ground Fault

- ii) During the fault, the Phase A voltage of the tidal site drops to 0.7 pu, the phase B voltage drops to 0.6 pu and the phase C voltage is maintained at 1 pu as seen from Figure 3.2.2 (b).

Due to fault in the 25 kV line, at time 5seconds the Phase A (Red) voltage starts falling to 0.7pu before increasing to 1pu at time 5.1 seconds. While at the same time, Phase B voltage (green) falls to 0.6pu and Phase C voltage maintains a steady 1pu.

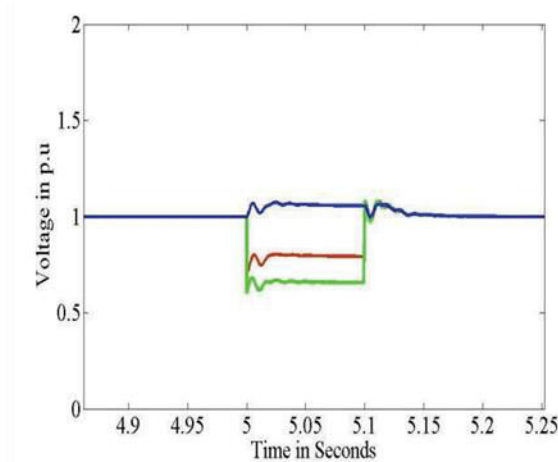


Figure 3.2.2 (b) Phase A Voltage drop fault

- iii) During the fault, the phase A voltage of the 25 kV line drops to zero, the phase B voltage increases to 1.01 pu and the phase C voltage increases to 1.22 pu as seen from Figure 3.2.2 (c).

Figure 3.2.2 (c) below shows at time 5 seconds, the phase A (Red) voltage falls to zero application of reactive power on the line. Meanwhile the Phase B (Green) and Phase C (Blue) increases at the same time with the same time 5 seconds and returns to 1pu after the fault at time 5.1 Seconds.

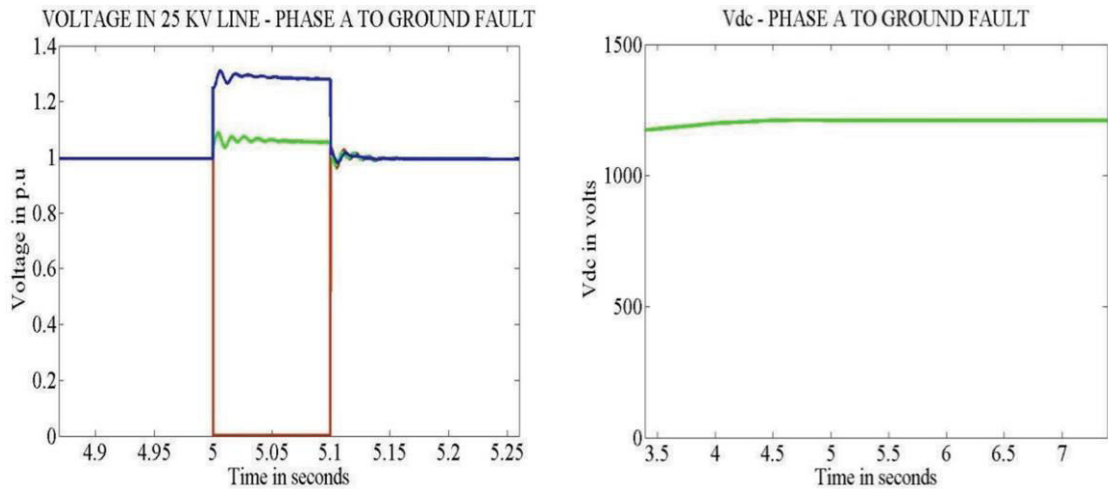


Figure 3.2.2 (c) Voltage in 25kV Line-Phase A to Ground Fault and Figure 3.2.2 (d) Vdc-Phase A To Ground Fault respectively

- iv) The value of Vdc is nearly 1200V as seen from Figure 3.2.2 (d). At this stage the Vdc is relatively steady at 1200V from 3.5 seconds because Phase A to ground fault has minimal or no effect on the DC voltage as shown in figure 3.2.2 (d).
- v) The generated real power undergoes fluctuations during the fault and which decreases from 1.2 MW to -0.2 MW at time 5.02 before increasing to 3.5 MW during the fault and recovers to the pre-fault value at 5.2 seconds as seen from in Figure 3.2.2 (e).
- vi) The generated reactive power increases smoothly to reach rated value of 4 MVAR during the fault period and reaches steady state value after 5.2 seconds as seen from Figure 3.2.2 (f).

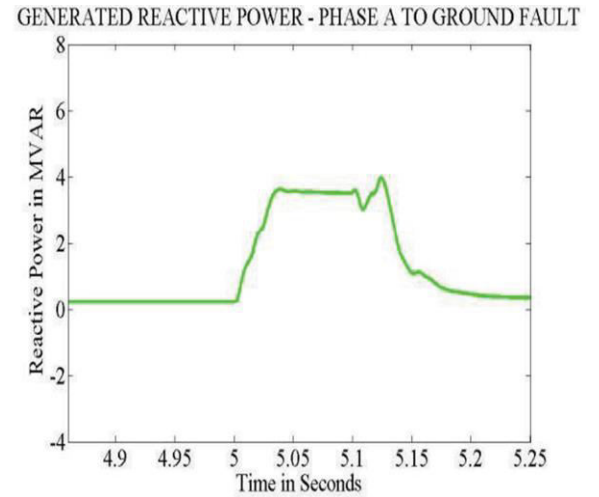
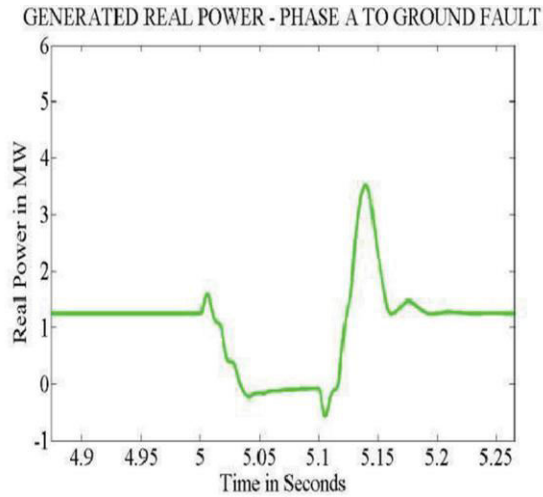


Figure 3.7(e) Generated Real Power-Phase A to Ground Fault and Figure 3.2.2 (f) Generated Reactive Power-Phase a to Ground Fault respectively

- vii) The real power in the 25 kV line increases to 6 MW during the fault and reaches steady value after 5.25 seconds as seen from Figure 3.2.2 (g).

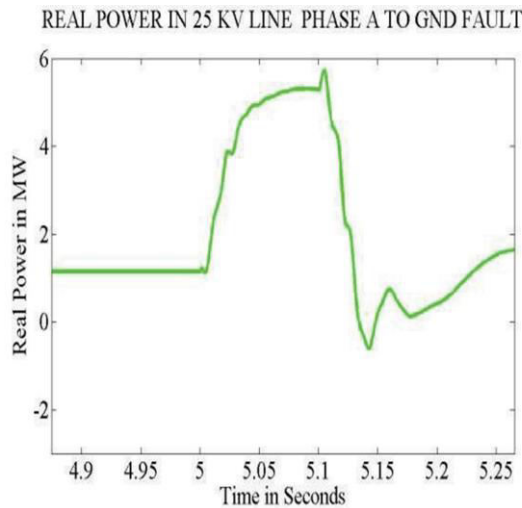


Figure 3.2.2 (g) Real Power in 25kV Line Phase A to Ground Fault.

- viii) The reactive power in the 25 kV line increases to 7.8 MVAR during the fault and reaches steady value after 5.25 seconds as seen from Figure 3.2.2 (h).

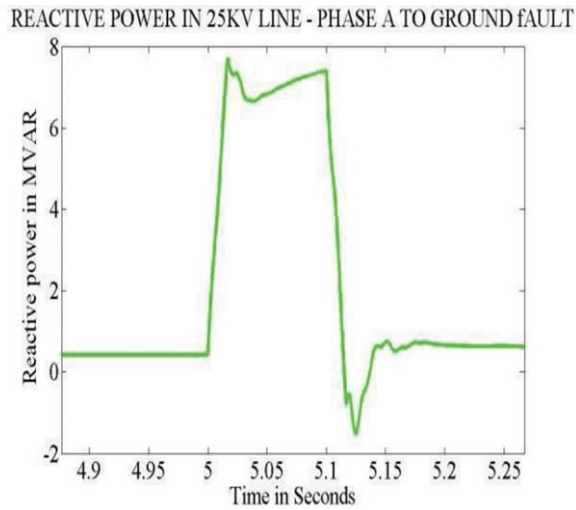


Figure 3.2.2 (h) Reactive Power in 25KV line-phase a to ground fault.

For a phase A and B fault in the 25 kV line for $t= 5$ to 5.1 seconds

- i) During the fault, the Phase A (red) voltage of the grid drops to 0.941 pu and phase B (green) and C (blue) voltage of the grid drops to 0.985 pu and as seen from *Figure 3.2.3 (a)*.

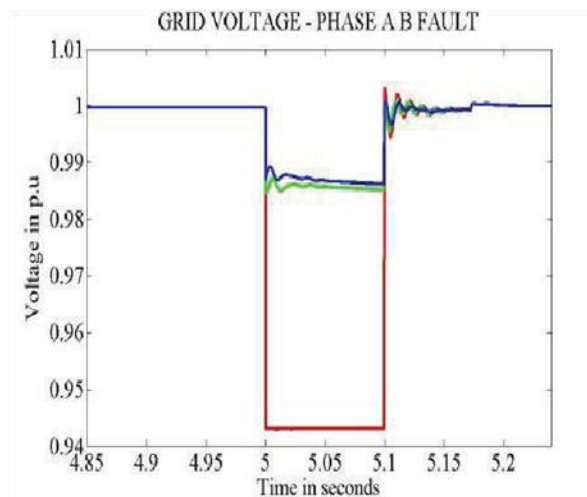


Figure 3.2.3 (a) Grid voltage-phase A B fault.

- ii) During the fault, the Phase A (red) voltage of the tidal power site drops to 0 pu and the phase B (green) and C (blue) voltages are maintained at 1 pu as seen from Figure 3.2.3 (b).

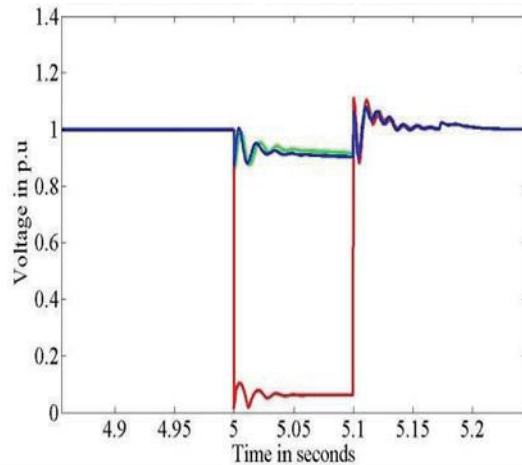


Figure 3.2.3 (b) Phase A Voltage fault during drops.

- iii) During the fault, the phase A (red) voltage of the 25 kV line drops to 0.5 pu, the phase B (green) and C (blue) voltages are maintained at 1 pu as seen from Figure 3.2.3 (c).

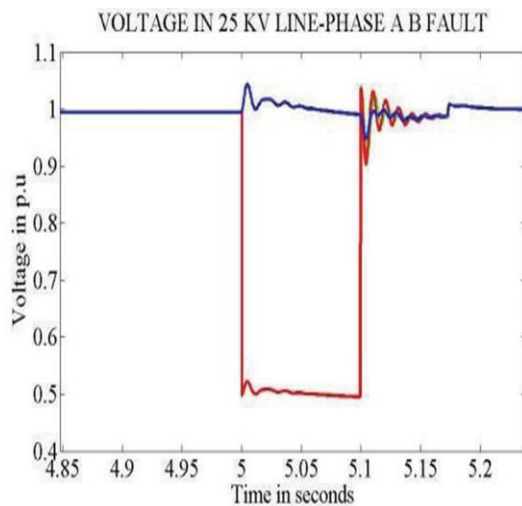


Figure 3.2.3 (c) Voltage in 25kV line-phase A B fault

- iv) The value of V_{dc} is nearly 1200V as seen from Figure 3.8 (d). In the graph in figure 3.2.3 (d) shows that the DC voltage becomes 1200V after back to back current conversion.

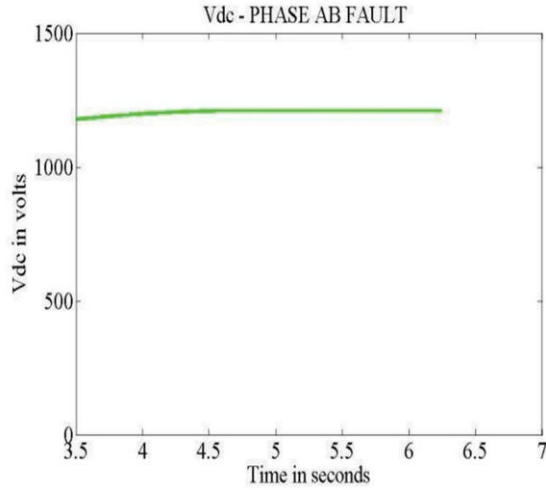


Figure 3.2.3 (d) Vdc Phase A B fault.

viii) The generated real power undergoes fluctuations and increases to 3.5 MW during the fault and recovers to the pre-fault value at 5.2 seconds as seen from *Figure 3.2.3 (e)*.

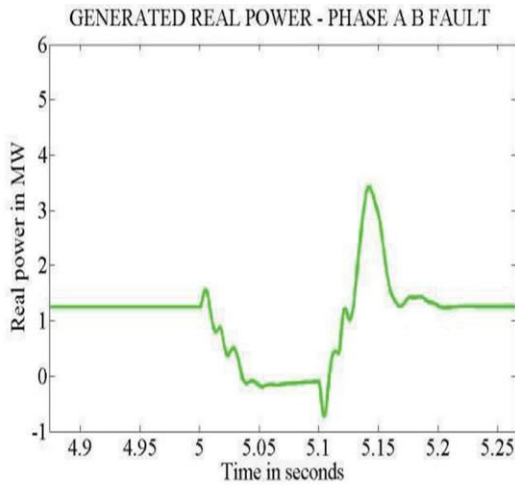


Figure 3.8 (e) Generated real power phase A B fault

v) The generated reactive power increases to 4.5 MVAR during the fault period and reaches steady state value of zero at 5.23 seconds as seen from *Figure 3.2.3 (f)*.

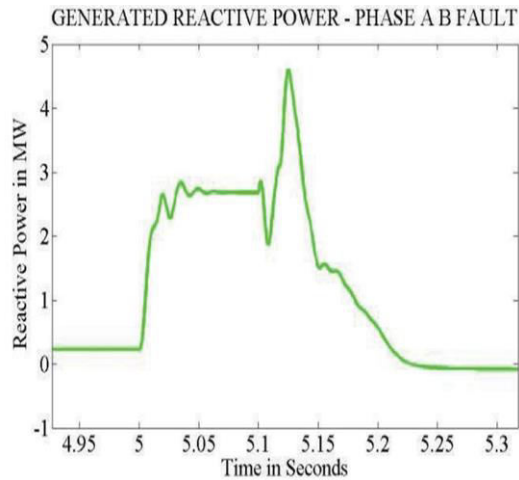


Figure 3.2.3 (f) Generated reactive power phase A B fault.

- vi) The real power in the 25 kV line increases to 4.1 MW during the fault and reaches steady value of -0.8 MW at 5.18 seconds as seen from Figure 3.2.3 (g).

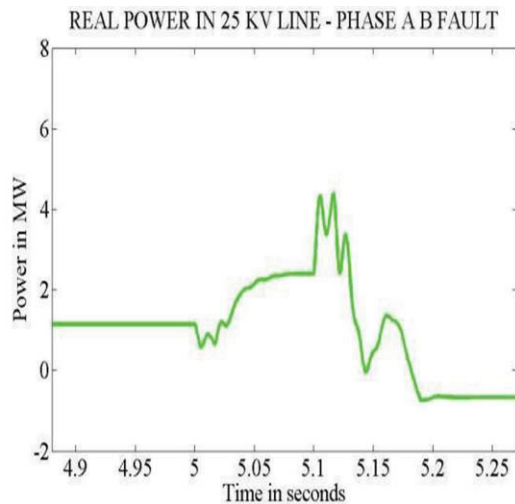


Figure 3.2.3 (g) Real power in 25kV line phase A B fault.

- vii) The reactive power in the 25 kV line increases to 2.1MVAR during the fault and reaches steady value of zero after 5.25 seconds as seen from Figure 3.2.3 (h). The graph in figure 3.2.3 (h) the reactive power remains steady until the fault is applied at time 5 seconds. The value of reactive power drops to -1.5MVAR and fluctuates and increases to 2.1 MVAR before reducing to reaching a steady state of zero value at time 5.18 seconds.

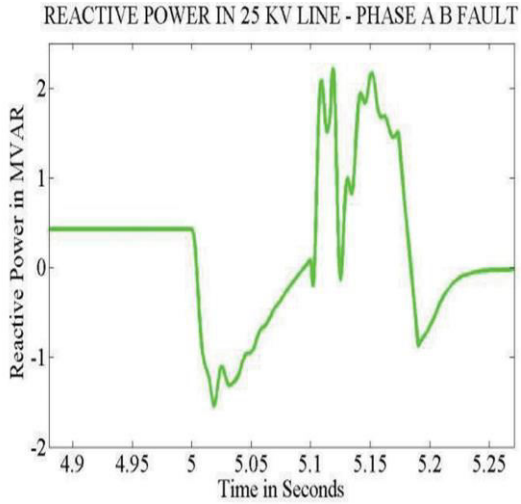


Figure 3.2.3 (h) Reactive power in 25kV line phase A B fault.

viii) The tidal speed varies from 8-13 m/s as shown in Figure 3.2.3 (i). The graph in figure 3.2.3 (i) shows that during the phase A and B in the line 25 kV, the tidal speed ranges from 8 to 13 m/s.

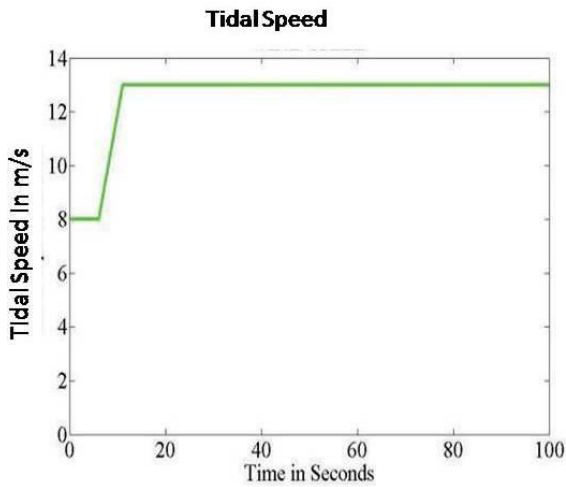


Figure 3.2.3 (i) Tidal Speed.

For a phase A and B to ground fault in the 25 kV line from $t = 5$ to 5.1 seconds

- i) During the fault, the Phase A (red) voltage of the grid drops to 0.941 pu and phase B (green) voltage of the grid drops to 0.98 pu and phase C (blue) voltage drops to 0.976 pu as seen from Figure 3.2.4 (a).

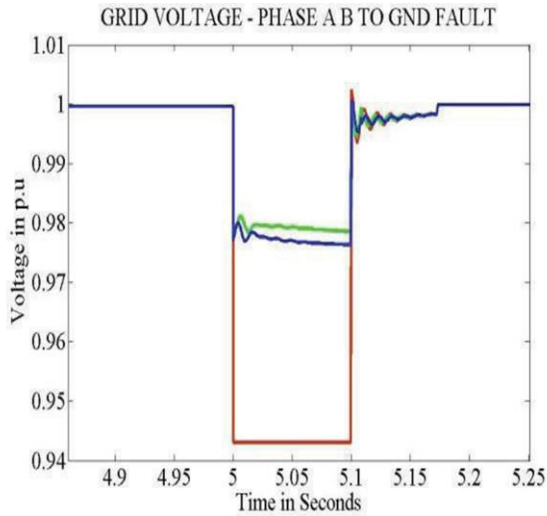


Figure 3.2.4 (a) Grid Voltage Phase A B to ground fault.

- ii) During the fault, the Phase B (green) voltage of the tidal site drops to 0.1 pu, the phase A (red) and C (blue) voltages drop to 0.8 pu as seen from Figure 3.2.4 (b).

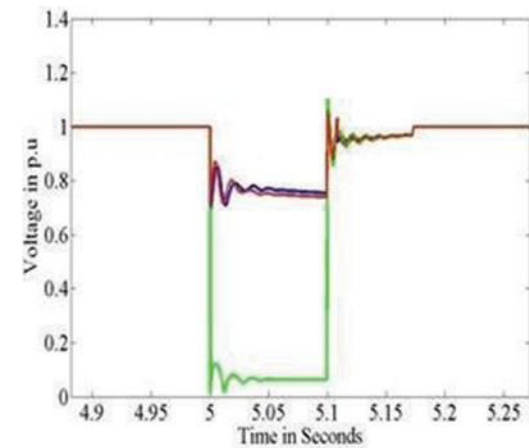


Figure 3.2.4 (b) Phase B voltage of the tidal site drops under fault

- iii) During the fault, the phase A (red) voltage of the 25 kV line drops to 0 pu, the phase B (green) and C (blue) voltages are maintained at 1.3 pu as seen from Figure 3.2.4 (c).

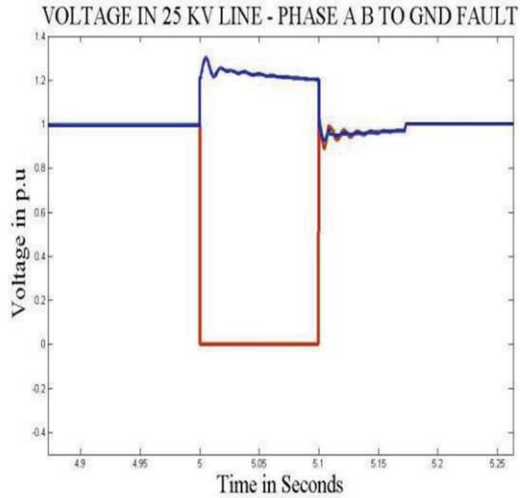


Figure 3.2.4 (c) Voltage in 25kV line phase A B to ground fault

iv) The value of Vdc is nearly 1200V as seen from Figure 3.2.4 (d).

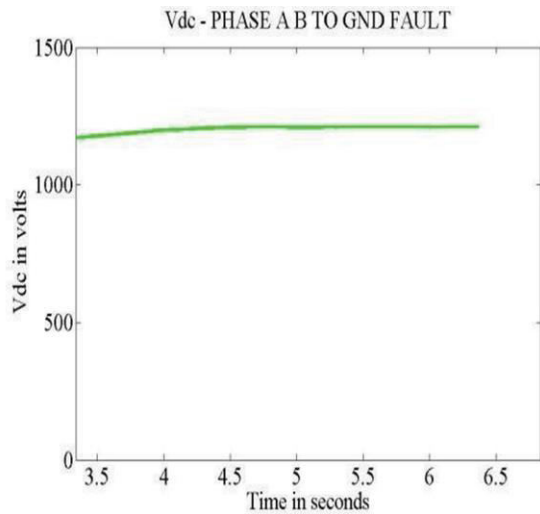


Figure 3.2.4 (d) Vdc Phase A B to ground fault.

v) The generated real power undergoes fluctuations and during the fault and reduces to zero at 5.2 seconds as seen from Figure 3.2.4 (e).

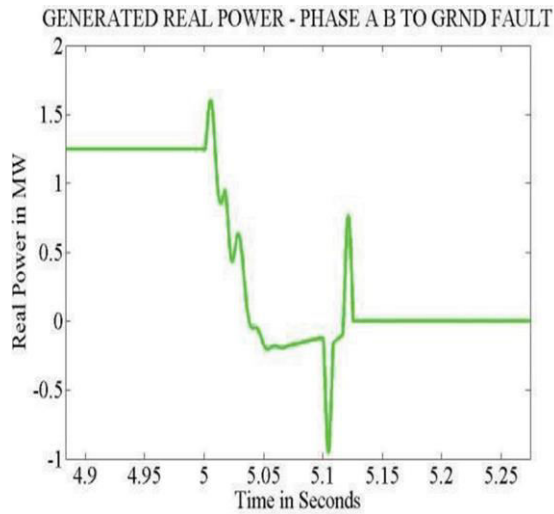


Figure 3.2.4 (e) Generated real power phase A B to ground fault.

- vi) The generated reactive power increases to 2.5 MVAR during the fault period and reaches steady state value of 0 MVAR at 5.2 seconds as seen from Figure 3.2.4 (f).

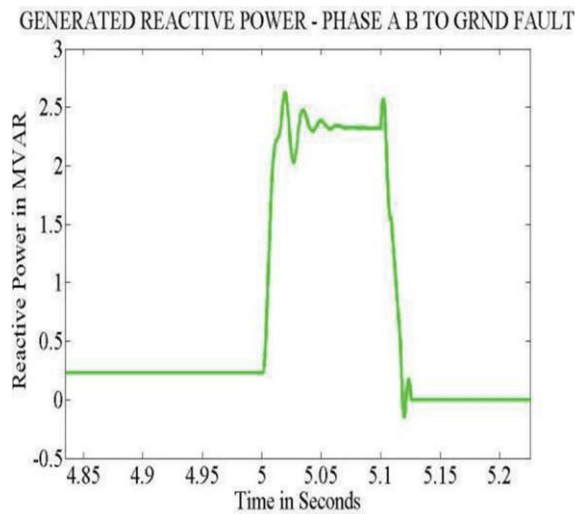


Figure 3.2.4 (f) Generated reactive power phase A B to ground fault.

- vii) The real power in the 25 kV line increases to 5.5 MW during the fault and reaches steady value of 0.5 MW at 5.18 seconds as seen from Figure 3.2.4 (g).

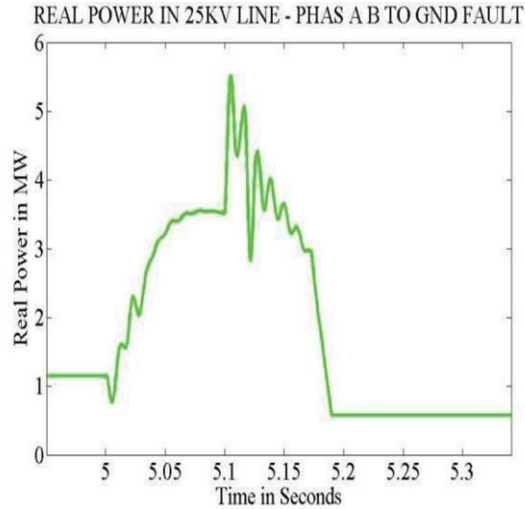


Figure 3.2.4 (g) Real power in 25kV line phase A B to ground fault.

- viii) The reactive power in the 25 kV line increases to 6.5 MVAR during the fault and reaches steady value of Zero at 5.18 seconds as seen from Figure 3.2.4 (h).

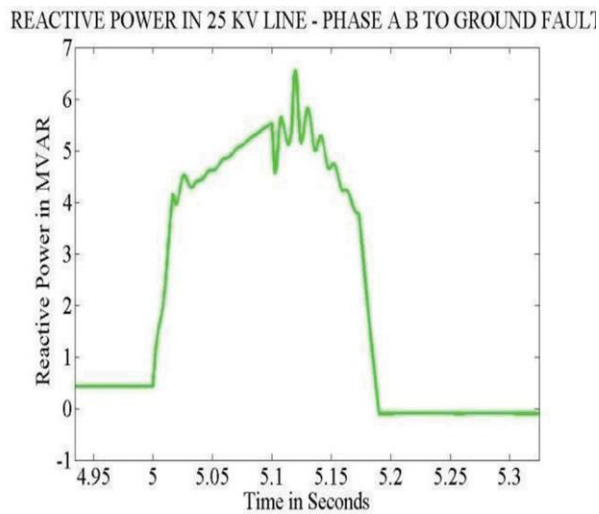


Figure 3.2.4 (h) Reactive power in 25kV line phase A B to ground fault.

For a Symmetric fault in the 25 kV line for $t= 5$ to 5.1 seconds

- i) During the fault, the Phase A, B and C voltages of the grid drops to 0.942 pu as seen from Figure 3.2.5 (a).

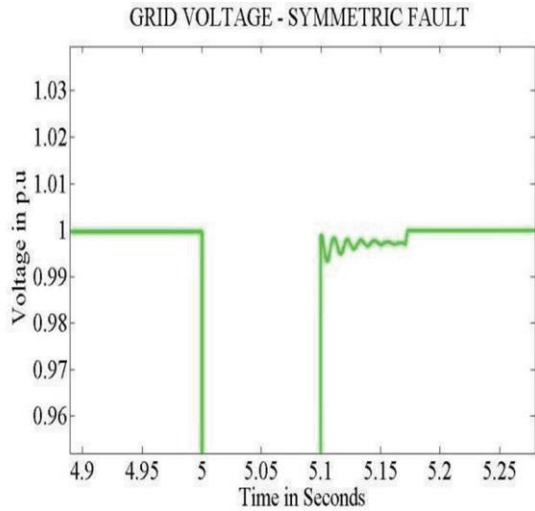


Figure 3.2.5 (a) Grid voltage-symmetric fault

- ii) During the fault, the Phase A, B and C voltages of the tidal site drops to 0 pu, as seen from Figure 3.2.5 (b).

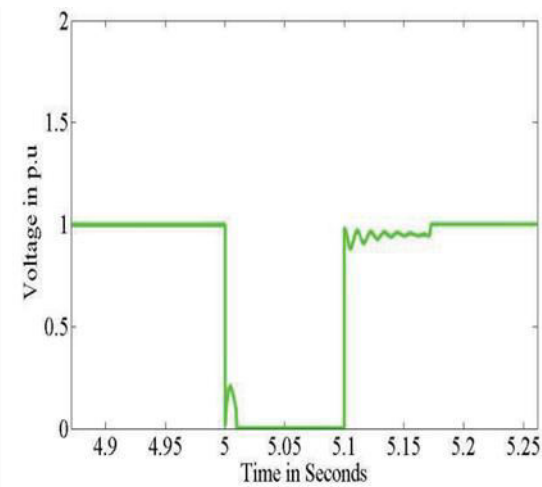


Figure 3.2.5 (b) Phase A, B and C voltages of the tidal site drops.

- iii) During the fault, the phase A, B and C voltages of the 25 kV line drops to 0 pu as seen from Figure 3.2.5 (c).

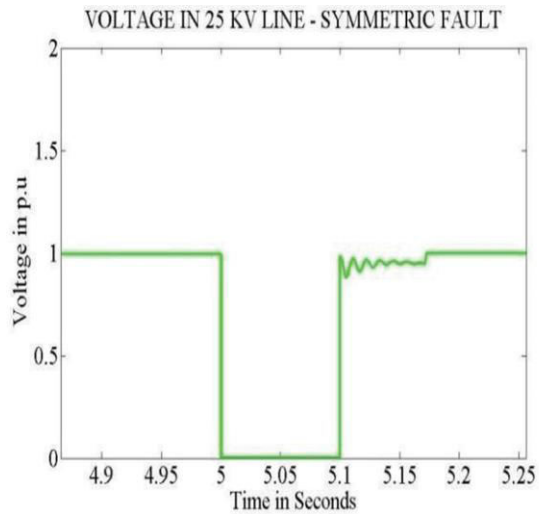


Figure 3.2.5 (c) Voltage in 25 kV line-symmetric fault

iv) The value of Vdc is nearly 1200V as seen from Figure 3.2.5 (d).

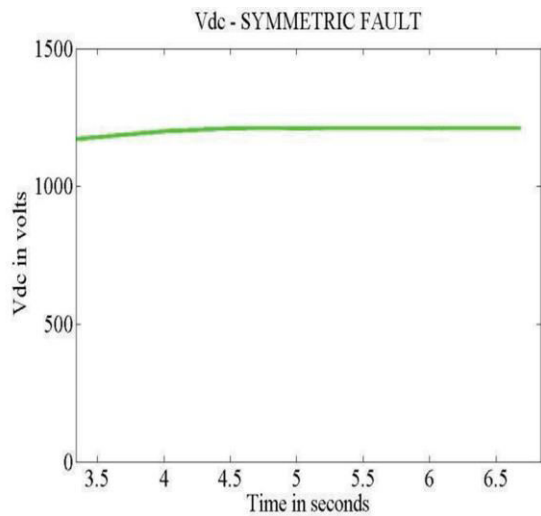


Figure 3.2.5 (d) Vdc-Symmetric fault

v) The generated real power reduces during the fault and reduces to zero at 5.03 seconds as seen from Figure 3.2.5 (e).

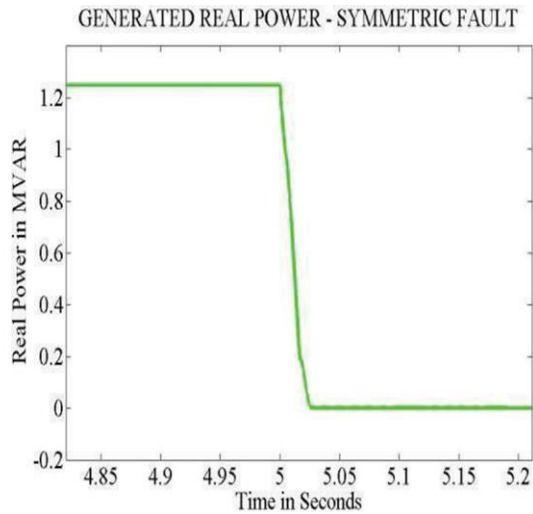


Figure 3.2.5 (e) Generated real power-symmetric fault

- vi) The generated reactive power increases during the fault period and reaches steady state value of 0 MVAR at 5.2 seconds as seen from Figure 3.2.5 (f).

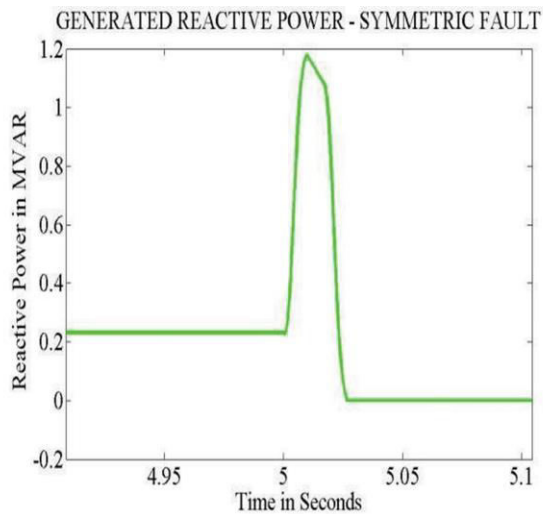


Figure 3.2.5 (f) Generated reactive power-symmetric fault.

- vii) The real power in the 25 kV line increases to 3.5 MW during the fault and reaches steady value of 0.6 MW at 5.18 seconds as seen from Figure 3.2.5 (g).

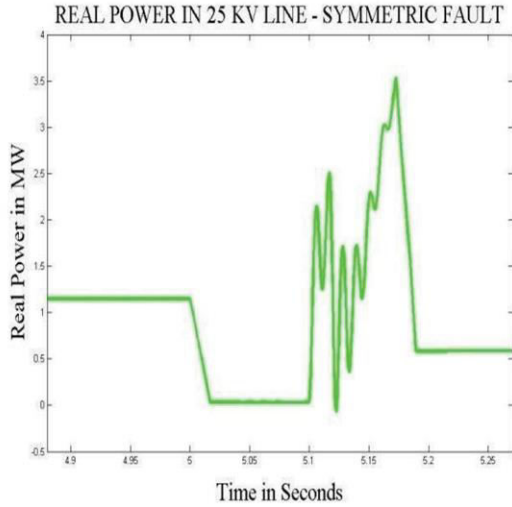


Figure 3.2.5 (g) Real power in 25kV line-symmetric symmetric fault.

- viii) The reactive power in the 25 kV line increases to 9 MVAR at 5.1 seconds during the fault and reaches steady value of Zero at 5.18 seconds as seen from Figure 3.2.5 (h).

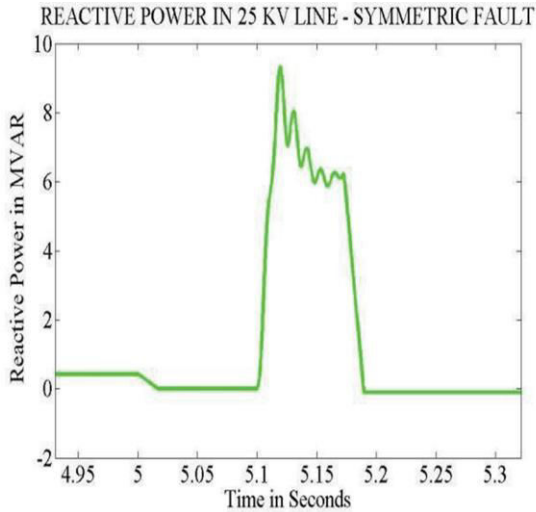


Figure 3.2.5 (h) reactive power in 25kV line-symmetric fault.

The fault analysis in 25 kV line of the tidal power site is analyzed in case there are open circuit which occurs if a circuit is interrupted by some failure. It is important to perform the above different faults because the three-phase step amplitude change can exceed the maximum voltage that the rotor converter can generate which causes current control to fail.

The graphics of stimulation results are given in V, W and Var to analysis the grid voltage, real power generated and reactive power respectively.

3.2.1 SUMMARY OF ANALYSIS

In this thesis work, a 6 MW Tidal Site using DFIG is simulated using MATLAB/ SIMULINK and the performance of the system is studied for normal condition and different fault conditions. The simulation results are presented and discussed. From the simulation results it can be inferred that the reactive power of the DFIG is controlled to maintain 1 pu voltage in the grid. For a phase A to ground fault on the 25 kV line, the real and reactive power from the tidal power site and the real and reactive power in the 25 kV line undergoes fluctuation during the fault period and is able to recover nearly at 5.15 seconds. The voltage in the 25 kV line and the Tidal Site output voltage settles to a steady state value at 5.13 seconds where as the grid voltage settles to a steady state value at 5.17 seconds. For phase A B fault, voltages settle to a steady state value at 5.17 seconds, where as the real and reactive power from the Tidal Site reaches steady state after fault recovery at 5.2 seconds. For phase AB to ground fault and symmetric fault, the generated real and reactive power and the reactive power in the 25 kV line falls to zero after the fault recovery.

CHAPTER FOUR

4.0 CONCLUSION

The use of tidal currents as a renewable source of energy is very effective as it relies on the same technologies used in offshore-wind generation and it is a more predictable source of energy. The thesis model used allows maximum energy extraction from oceans tides for low tidal speed using doubly fed induction generator technology. DFIG technology is also used to minimize mechanical stresses on the turbine.

Tides play a very important role in the formation of global climate as well as the ecosystems for ocean inhabitants. At the same time, tides are a substantial potential source of clean renewable energy for future human generations. Depleting oil reserves, the emission of greenhouse gases by burning coal, oil and other fossil fuels, as well as the accumulation of nuclear waste from nuclear reactors will inevitably force people to replace most of our traditional energy sources with renewable energy in the future. Tidal energy is one of the best candidates for this approaching revolution. Development of new, efficient, low-cost and environmentally friendly hydraulic energy converters suited to free-flow waters, such as triple-helix turbines, can make tidal energy available worldwide. This type of machine, moreover, can be used not only for multi-megawatt tidal power farms but also for mini-power stations with turbines generating a few kilowatts. Such power stations can provide clean energy to small communities or even individual households located near continental shorelines, straits or on remote islands with strong tidal currents. Further research can also be done using Permanent Magnet Synchronous Generator (PMSG) instead of using DFIG.

Simulations indicate that design parameters and control parameters have impacts on the lifespan of the system. Studies on the lifespan sensitivity to these parameters will provide directions for designers. To enhance the scale of tidal system, interconnection of tidal generators is a trend. Tidal generators are sequentially and spatially correlated because tidal current flows from one generator to another. How to coordinate the generators to extend lifespan of the whole system will also become a research direction.

REFERENCES

1. ACRE (1999), Tidal power systems, <http://acre.murdoch.edu.au/refiles/tidaltxt.html>. Australian CRC for Renewable Energy, Alternative Energy Development Board. An Introduction to Signal Detection and Estimation, New York: Springer-Verlag, 1985, ch. 4. (Book Chapter)
2. Tidal Electric. History of Tidal power. <http://www.tidalelectric.com/History.htm>
3. T. J. Hammons, "Accumulative Fatigue Life Expenditure of Turbine/Generator Shafts Following Worst-Case System Disturbances," *IEEE Trans. Power Apparatus and Systems*, vol.PAS-101, no.7, pp.2364-2374, July 1982.
4. Clare, R, 1992. Tidal power trends and development. Thomas Telford ,Londo E. Kaba1cl, E. Irmak, 1. C:olak, "Design of an AC-DC-AC converter for wind turbines", *International Journal of Energy Research*, Wiley Interscience, DOI: 10.1002/er.1770, Vol. 36, No. 2, pp. 169-175. (Article)
5. Blue Energy (2001) Blue Energy Canada Inc., Vancouver, Canada (formerly known as Nova Energy)
6. Tidal Power, DIL-HM group. Information available at <http://dil.hmgroups.com/ltidal.html>
7. Ltd.,(Nova Scotia)IEEE Standard 519-1992, Recommended practices and requirements for harmonic control in electrical power systems, The Institute of Electrical and Electronics Engineers, 1993. (Standards and Reports)
8. HM Treasury and DETR press release (2000) Protecting the Environment and Supporting Britain's Road Transport, UK Parliament, 7th March 2001.
9. Yunus, M. 1998. Poverty Alleviation: Is Economics Any Help. Lessons from the Grameen Bank Experience. *Journal of International Affairs* 52(1):50-51.
10. ESCAP. 1998. Energy Issues and Prospects in the Asia and Pacific Region. Economic and Social Commission for Asia and the Pacific of United Nations, New York, USA
11. Underwood, AJ. and Chapman, M.G. 1999. The role of ecology in coastal zone management: Perspectives from South-east Australia. In *Perspectives on integrated coastal zone management*, edited by W. Salomons, R.K. Turner, L.D. DeLacerda and S. Ramachandran, 99- 128. Berlin: Springe.
12. V. Akhmatov, "Analysis of dynamic behavior of electric power system with large amount of wind power," Ph.D. dissertation, Technical University of Denmark, 2003.

13. I. Erlich, J. Kretschmann, J. Fortmann, S. Mueller-Engelhardt, and H. Wrede, "Modeling of wind turbines based on doubly-fed induction generators for power system stability studies," *IEEE Transactions on Power Systems*, vol. 22, no. 3, pp. 909 – 919, Aug. 2007.
14. P. Ledesma and J. Usaola, "Doubly fed induction generator model for transient stability analysis," *IEEE Transactions on Energy Conversion*, vol. 20, no. 2, pp. 388 – 397, Jun. 2005.
15. Y. Lei, A. Mullane, and G. Lightbody, "Modelling of the wind turbine with a doubly fed induction generator for grid integration studies," *IEEE Transactions on Energy Conversion*, vol. 21, no. 1, pp. 257 – 264, Mar. 2006.
16. N. Miller, J. Sanchez-Gasca, W. Price, and R. Delmerico, "Dynamic modeling of GE 1.5 and 3.6 MW wind turbine-generators for stability simulations," in *Proceeding of Power Engineering Society General Meeting*, vol. 3, Jul. 2003, pp. 1977 – 1983
17. K. Clark, N. Miller, W. Price, and J. Sanchez-Gasca, "Modeling of GE wind turbine-generators for grid studies," General Electric International, Inc., Technical Report, Jan. 2008.
18. Calderon, EJ. and Alvarez-Villamil, G. 2000. Sustainability in Rural and Coastal Areas: The role and impact of infrastructure in rural and coastal areas. Intergovernmental Oceanographic Commission, the National Ocean Service, the World Bank, and the Center for the Study of Marine Policy, the University of Delaware, USA, [www.coastalmanagement.com]
19. Causes of high tide and low tide. Information is available at <http://science.howstuffworks.com/environmental/earth/geophysics/tide-cause.htm>
20. Spring tides and Neap tides. <http://www.almanac.com/content/spring-tides-neap-tides>
21. Tides and Tidal currents, National Imagery and Mapping Agency Publication. http://msi.nga.mil/MSISiteContent/StaticFiles/NAV_PUBS/APN/Chapt-09.pdf
22. Donald E. Simanek, Tidal Misconceptions (2003). <http://www.lhup.edu/~dsimanek/scenario/tides.htm>
23. Gravitational tides. <http://burro.astr.cwru.edu/Academics/Astr221/Gravity/tides.html>
24. The Ocean's Tides. <http://www.moonconnection.com/tides.phtml>
25. Yun Seng. Lim and Siong Lee. Koh (2009). Marine Tidal Current Electric Power Generation: State of Art and Current Status, Renewable Energy, T J Hammons (Ed.),

ISBN: 978-953-7619-52-7, In Tech, Available from:
<http://www.intechopen.com/books/renewable-energy/marine-tidal-current-electric-power-generation-state-of-art-and-current-status>

26. Tidal stream generator. http://energyeducation.ca/encyclopedia/Tidal_stream_generator
27. Power conversion System Design For Tidal Stream Generators. <http://www.optimacs.com/wp-content/uploads/2012/03/Power-conversion-system-design-for-tidal-stream-generator-approved.pdf>
28. Using the power of the tidal streams to generate electricity. http://www.google.de/imgres?imgurl=http://www.alternative-energy-tutorials.com/images/stories/tidal/alt93.gif&imgrefurl=http://www.alternative-energy-tutorials.com/tidal-energy/tidal-stream.html&h=327&w=421&tbnid=QyIPeZ35RhqWuM:&tbnh=90&tbnw=116&usg=__thrasMrK-2tvAXgkmEow9mI8MJM=&docid=tDED7bJF9L7wJM&sa=X&ved=0CCYQ9QEwAGoVChMI9s7C6Z7JyAIVShAsCh1vSQDU
29. Tidal Power. http://www.esru.strath.ac.uk/EandE/Web_sites/01-02/RE_info/Tidal%20Power.htm#barrage
30. Tidal Barrages. http://www.tidalenergy.eu/tidal_barrages.html
31. TidalEnergyTechnologyBrief, International RenewableEnergyAgency. http://www.irena.org/DocumentDownloads/Publications/Tidal_Energy_V4_WEB.pdf
32. Dynamic Tidal Power (DTP). <http://tidalpower.co.uk/dynamic-tidal-power>
33. Advantages and Disadvantages of Tidal Power. <http://thenextgalaxy.com/the-advantages-and-disadvantages-of-tidal-energy-power/>
34. Dynamic Tidal Power (DTP). <http://www.green-mechanic.com/2014/06/dynamic-tidal-power.html>
35. List of Tidal Power Plants and Future Tidal Stations-Facing Difficult Times. <http://www.greenworldinvestor.com/2011/03/13/list-of-tidal-power-plants-and-future-tidal-stations-facing-difficult-times/>

36. Hotta, K. and Dutton, I.M. 1995. Coastal Management in the AsiaPacific Region: Issues and Approaches. Japan International Marine Science and Technology Federation, Tokyo, Japan.
37. Gill, A. 2005. Offshore renewable energy: Ecological implications of generating electricity in the coastal zone. *Journal of Applied Ecology*, 42:605-615.
38. DOE (U.S. Department of Energy). 2009. *Report to Congress on the Potential Environmental Effects of Marine and Hydrokinetic Energy Technologies: Prepared in Response to the Energy Independence and Security Act of 2007, Section 633(B)*. Wind & Power Program, Energy Efficiency & Renewable Energy, U.S. Department of Energy. December 2009.
39. MMS (Minerals Management Service). 2007. *Programmatic Environmental Impact Statement for Alternative Energy Development and Production and Alternate Use of Facilities on the Outer Continental Shelf*. U.S. Department of the Interior. OCS EIS/EA MMS 2007-046. October 2007.
40. Bryans, A. G., Fox, B., Crossley, P. and O'Malley, M. J., "Impact of tidal generation on power system operation in Ireland", *IEEE Transactions on Power Systems*, 20 (4), 2034–2040, .2005.
41. Denny, E., "The economics of tidal energy", *Energy Policy*, 37, 1914– 1924, 2009.
42. Lefton, S., Besuner, P., "Power plant cycling operations and unbundling their effect on plant heat rate" APTECH Technical Paper TP134 - <http://www.aptecheng.com>, 2001.
43. Denny, E., O'Malley, M., "The impact of carbon prices on generation cycling costs", *Energy Policy*, 37, 1204-1212, 2009.
44. Denny, E., O'Malley, M., "Quantifying the total net benefits of grid integrated wind", *IEEE Transactions on Power Systems*, 22 (2), 605–615, 2007.
45. Denny, E., "The economics of tidal energy", *Energy Policy*, 37, 1914–1924, 2009.
46. All Island Project (AIP), "Single electricity market – fixed cost of a best new entrant peaking plant for the calendar year 2009", <http://www.allislandproject.org>